MOTION AND BLOOD FLOW IN THE CARPAL TUNNEL

INVESTIGATING THE EFFECTS OF ALTERED BLOOD FLOW, FORCE, WRIST POSTURE, FINGER MOVEMENT SPEED, AND POPULATION ON MOTION AND BLOOD FLOW IN THE CARPAL TUNNEL

By ANDREW Y.W. WONG, BSc

A Thesis Submitted to the School of Graduate Studies in Partial Fulfilment of the Requirements for the Degree Master of Science

McMaster University MASTER OF SCIENCE (2021) Hamilton, Ontario (Science)

TITLE: Investigating the effects of altered blood flow, force, wrist posture, finger movement speed, and population on motion and blood flow in the carpal tunnel

AUTHOR: Andrew Y.W. Wong, BSc (McMaster University) SUPERVISOR: Dr. Peter Keir, PhD NUMBER OF PAGES: xv, 90

LAY ABSTRACT

This thesis aimed to evaluate and summarize key findings from the McMaster Occupational Biomechanics Laboratory relating to tissue motion and blood flow in the carpal tunnel. Performing repetitive finger movements faster and with a flexed wrist posture were found to decrease the distance travelled of the underlying finger tendon. Blood flow of the median nerve, which is implicated in carpal tunnel syndrome (CTS), is higher with forceful exertion and flexed wrist posture, and lower with greater severity of CTS. Finally, altering blood flow to the carpal tunnel was found to create a CTS-like environment, affected tissue motion in the carpal tunnel, and promoted movement disparity between these tissues that is associated with injury. This suggests that fluid/blood flow changes affecting the carpal tunnel is a plausible mechanism for increasing the likelihood of developing CTS.

ABSTRACT

Data from the McMaster Occupational Biomechanics Laboratory were consolidated to evaluate overall trends relating to tissue motion and blood flow in the carpal tunnel. Regarding tissue motion, displacements of the flexor digitorum superficialis (FDS) tendon and its subsynovial connective tissue (SSCT) were found to decrease with greater movement speed and a flexed wrist posture. Notably, changes to shear outcomes including relative tendon-SSCT displacement, the shear strain index (SSI), and maximum velocity ratio (MVR) demonstrate that greater movement speed contributes to SSCT damage according to the shear strain mechanism of injury theorised to promote carpal tunnel syndrome (CTS). Median nerve blood flow was also found to be implicated by wrist flexion, and appeared to decrease with greater CTS severity status. Finally, induced blood flow alteration of the carpal tunnel was found to elicit a median nerve blood flow response similar to the level found in CTS subjects, confirming its effectiveness as an intervention to study tissue motion in a CTS-like state. The influence of altered blood flow on tissue motion was differential, where the higher supradiastolic condition altered FDS displacement, and the lower subdiastolic condition affected SSCT displacement and SSI. These findings provide valuable evidence for changes in median nerve blood flow—and by extension, the local fluid environment within the carpal tunnel—not only being a consequence of SSCT fibrosis characteristic of CTS, but potentially also acting as a cause for said changes in carpal tunnel tissue motion.

ACKNOWLEDGEMENTS

To say this journey was anything but a wild ride would be an understatement. Not only was I tested in the academic sense, but on a mental and emotional level as well. Somehow, I've made it out the other side—and these are some of the people I'd like to thank for assisting me along the way.

First, to my supervisor, Dr. Peter Keir. People are often the product of their surroundings and of the people they surround themselves with. By some miracle, and through my interest in this field, I was able to grow from an undergrad in the lab to a successfully completed graduate student under your supervision. There were some bumps along the way, but we did it. We might not get the full experience with the whole supervisor-student sash routine at convocation, but your congratulations and approval mean just as much. Thank you, Pete, for helping me throughout all these years—for giving me confidence when I didn't have any, for being patient with me, and for providing me with more support than I've probably ever received from a single person. Most importantly, beyond the research skills and biomechanics knowledge, thank you for helping me become a slightly better person that will hopefully continue to show compassion and kindness to others, just as you do.

To my friends from the lab: thank you for welcoming me when I was a starry-eyed undergrad, to an incredibly lost grad student. To Dan Mulla, you've always been exceptionally kind to me and helped me through so many concepts…and confused even more on others. I am eternally grateful you've been there for me every step of the way throughout my time in the lab. To Amanda Farias Zuniga, thank you for being a mentor,

for being understanding, and for being my partner-in-crime for CTS-related topics in the lab. Hopefully I've made you somewhat proud of me, of my progress as both a scientist and as a person. To Kumar Somasundram, thank you for being a friend, and for teaching me how to write a for-loop when I needed to use MATLAB. I ended up copy-pasting most of my code anyways, but it could have been much, much worse without your help. To Riley Craig, thank you for being with me every step of the way throughout our time as grad students. Whenever I felt completely lost with an assignment or behind on one thing or another, you always supported me and reminded me I wasn't in it alone. Sometimes we'd joke that if we were to fail, at least we'd fail together, but we made it and are both finally done. To Kevin Kos, I am eternally jealous of your programming capabilities, but am even more grateful you've always been willing to help us out in our studies. Thank you for being such a positive member of our lab. To Brittany Bulbrook, thank you for being supportive, especially when I was struggling. Whether during my undergrad or throughout grad school, you've always been kind to me. Most importantly, you've always reminded me there's more to life than school, and now that I'm done, I can finally take a page out of your book and try to live life to the fullest. To Tony Gatti, thank you for always teaching me so much about stats, for being patient and helping me with assignments when you absolutely didn't need to, and for taking walks with me to clear my mind. I'm happy we've become close and am devastated you're so far away now, but hopefully we'll see each other again someday.

Next, to friends. To Lin Ke and Gloria Shao: thank you both for being supportive of me throughout this degree. Lin, I've known you since high school and you've always

shown me kindness and have helped me through countless tough times, whether you're aware of it or not. I will always be grateful that you try to invite me to go out, even when I can't always show up. Gloria, I've only gotten to know you recently, but thank you so much for being such a kind and open person. I'm really glad that we've become friends—please give Taro some catnip for me. To Mai Wageh: you are such a bright and beautiful person inside and out. Thank you for being so welcoming to me when I was a fresh grad student. Even though I'd already been in the department in my undergrad, you helped make the start of my grad student experience so much less daunting than it was, simply by being a friend to me. To Laura St. Germain: somehow, we both spent time at the same high school, but were never there at the same time. Thankfully, I was able to finally meet you at McMaster, and am so lucky to be able to call you my friend. You're exceptionally kind and are always such a pleasure to be around. To Sitara Sharma: evening strolls in DBAC were always great when I got to chat with you. I can't decide what you excel at more: your eye for art, or your capacity for kindness. Thank you for your support, especially throughout this pandemic. To Caitlin Sherry: it has always been a welcome surprise bumping into you during a commute. It's fun to think back to the time we were stuck late at night, in the middle of Hamilton, because of a snowstorm. I wouldn't have wanted any other person to go through all those bus delays with. You are a joy to be around, and I hope we can catch up again soon. To Madelaine Jong: you've shown me incredible kindness over the years, helped me normalize feeling okay on my birthday, and shown me unmatched compassion during one of the darkest points in my life. I will always be grateful to have met you during my undergrad. To Natalie Chan: you'll always

be my favourite lab partner. Thank you for always being open to going on adventures with me, for having such a wonderful sense of humour, and for helping me grow to be the person I am today. I miss you lots and hope to catch up soon. To Mirette Mounir: you are such an exceptionally kind, driven individual, that I also somehow get to call my friend. The only thing more astounding than your work ethic is your amazing personality. Thank you for supporting me throughout this pandemic, and for pushing me to finish my thesis when I doubted myself. Last but not least, to Taylor Wilkins: somebody I consider to be one of my closest friends. You've been there for me from the very first day of undergrad, and all the way throughout my Master's degree. From every accomplishment to every struggle, I could always count on your honesty and support. It absolutely means the world to me that you've been there every step of the way during my time at McMaster. You are possibly the most amazing, kind-hearted person I know, and I am so thankful we are friends.

Finally, to my grandpa, 爷爷, who passed away before seeing me complete my Master's.

TABLE OF CONTENTS

1. Introduction 1
2. Literature Review 2
   2.1) Carpal Tunnel Overview 2
   2.2) Carpal Tunnel Pressure 3
   2.3) Subsynovial Connective Tissue 4
   2.4) Implications of Movement Speed on Carpal Tunnel Structures 8
   2.5) Median Nerve 9
   2.6) Median Nerve Blood Flow with CTS 11
   2.7) Biomechanical Influences on Median Nerve Blood Flow 13
   2.8) Considerations due to Biological Sex 14
   2.9) Altered Fluid and Median Nerve Blood Flow in the Carpal Tunnel 15
3. Purpose 17
4. Hypotheses 17
5. Methods 18
   5.1) Biomechanical Influences on Tendon and SSCT Motion 18
      5.1.1) Finger Movement Speed 20
      5.1.2) Deviated Wrist Postures 20
   5.2) Median Nerve Blood Flow Changes 21
      5.2.1) Biomechanical Influences on Median Nerve Blood Flow 21
      5.2.2) Group Differences 22
   5.3) Effect of Induced Blood Flow Alteration 24
      5.3.1) Tendon and SSCT Motion 24
      5.3.2) CTS Comparison 25
   5.4) Statistics 26
6. Results 27
   6.1) Biomechanical Influences on Tendon and SSCT Motion 27
      6.1.1) FDS Displacement 27
      6.1.2) SSCT Displacement 29
      6.1.3) Strain Measures 30
   6.2 Median Nerve Blood Flow Changes 33
      6.2.1) Biomechanical Influences on Median Nerve Blood Flow 33
      5.2.2) Group Differences 35
   6.3) Effect of Induced Blood Flow Alteration 37
      6.3.1) Tendon and SSCT Motion 37
      6.3.2) CTS Comparison 41

7. Discussion 42
7.1) Biomechanical Influences on Tendon and SSCT Motion 42
7.1.1) FDS Displacement 42
7.1.2) SSCT Displacement 44
7.1.3) Strain Measures 44
7.2) Median Nerve Blood Flow Changes 45
7.2.1) Biomechanical Influences on Median Nerve Blood Flow 45
7.2.2) Group Differences 46
7.3) Effect of Induced Blood Flow Alteration 48
7.4) Limitations 49
8. Conclusion 50
9. References 51
10. Appendices 58
Appendix 1 58
Appendix 2.1 62
Appendix 2.2 63
Appendix 2.3 64
Appendix 2.4 65
Appendix 2.5 66
Appendix 2.6 67
Appendix 2.7 68
Appendix 2.8 69
Appendix 2.9 70
Appendix 2.10 71
Appendix 3.1 72
Appendix 3.2 73
Appendix 3.3 74
Appendix 3.4 75
Appendix 3.5 76
Appendix 3.6 77
Appendix 4.1 78
Appendix 4.2 79
Appendix 4.3 80

Appendix 4.4 81
Appendix 4.5 82
Appendix 4.6 83
Appendix 4.7 84
Appendix 4.8 85
Appendix 4.9 86
Appendix 4.10 87
Appendix 4.11 88
Appendix 4.12 89

LIST OF FIGURES AND TABLES

Figure 2.1.1. Boundaries of the carpal tunnel 2

Figure 2.1.2. Cross section of the carpal tunnel and its contents..... 3

Figure 2.3.1. SSCT blood vessel with motion 7

Table 5.1. Sample and analysis details for investigation of biomechanical influences on tendon and SSCT motion..... 19

Table 5.2. Sample and analysis details for investigation of biomechanical influences on median nerve blood flow velocity (BFV)..... 22

Table 5.3. Sample and analysis details for investigation of CTS status on median nerve blood flow velocity (BFV)..... 23

Table 5.4. Breakdown of CTS status levels used to predict median nerve blood flow for each model..... 23

Table 5.5. Sample and analysis details for investigation of local blood flow alteration on tendon and SSCT motion..... 24

Table 5.6. Breakdown of CTS status levels used to predict median nerve blood..... 25

Figure 6.1. FDS Displacement results for velocity and wrist posture 27

Table 6.1. Model results for FDS and SSCT displacements..... 28

Figure 6.2. SSCT Displacement results for velocity and wrist posture..... 29

Figure 6.3. Strain measures by FDS velocity (left) and SSCT velocity (right). 31

Table 6.2. Model results for shear measures (relative displacement, SSI, and MVR).... 32

Figure 6.4. Median nerve blood flow velocity by a) wrist posture and b) force 33

Table 6.3. Model results for median nerve (MN) blood flow velocity (BFV) 34

Figure 6.5. Median nerve blood flow velocity by CTS status 35

Table 6.4. Model results for median nerve blood flow velocity (BFV) with CTS Status, CTS Status 2 (where CTS is separated into its severities), and Symptoms as predictors .. 36

Figure 6.6. Tissue displacements by altered blood flow (left column) and altered blood flow type (right column) 38

Table 6.5. Model results for changes in tissue motion from altered blood flow..... 39

Table 6.6. Model results for changes in strain measures from altered blood flow 40

Figure 6.7. Median nerve blood flow velocity for different CTS Status groups 41

LIST OF ABBREVIATIONS AND SYMBOLS

BFV	Blood Flow Velocity
CTP	Carpal Tunnel Pressure
CTS	Carpal Tunnel Syndrome
DBP	Diastolic Blood Pressure
DIP	Distal Interphalangeal
FDP	Flexor Digitorum Profundus
FDS	Flexor Digitorum Superficialis
MCP	Metacarpophalangeal
MN	Median Nerve
MVR	Maximum Velocity Ratio
PIP	Proximal Interphalangeal
SBP	Systolic Blood Pressure
SSCT	Subsynovial Connective Tissue
SSI	Shear Strain Index
TCL	Transverse Carpal Ligament

DECLARATION OF ACADEMIC ACHIEVEMENT

Research contributions accomplished by this thesis include evaluating years of carpal tunnel syndrome research from the McMaster Occupational Biomechanics Laboratory and summarising the overall findings. Additionally, the feat of combining data from multiple studies to determine significance of results, interpreting the physiological phenomena, and forming comparisons to the literature is incredibly valuable for understanding the underlying mechanism for carpal tunnel syndrome. Finally, the thesis demonstrated the viability of blood flow changes in the carpal tunnel as not just a consequence of carpal tunnel syndrome, but perhaps a potential instigator as well.

1. Introduction

Carpal tunnel syndrome (CTS) is the most common peripheral neuropathy and the result of median nerve entrapment in the carpal tunnel of the wrist. Symptoms of CTS include pain, numbness, and tingling in the hand and fingers (Atroshi et al., 1999). CTS carries a financial impact of approximately $2 billion annually in the United States (Dale et al., 2013). The prevalence of CTS has been estimated to range from 4% in the general population (Atroshi et al., 1999) to 8% in the US working population, with a higher proportion of cases owing to females (10%) compared to males (6%) (Dale et al., 2013). While median nerve compression characterizes CTS, the events leading up to and are responsible for this outcome are not as well understood. Associations have been made between occupational exposures to CTS development such as computer use in offices (Shiri & Falah-Hassani, 2014), high forces and repetitive work in industrial settings (Silverstein, Fine, & Armstrong, 1987), and raw meat processing in poultry plants (Musolin & Ramsey, 2017). However, the necessity of understanding the underlying task components that contribute to these associations cannot be understated. Chronic exposure to occupational risk factors including excessive force, repetitive exertions, and non-neutral postures have been linked to an increased risk for developing CTS (Keir et al., 2019). These factors can increase the hydrostatic pressure acting against the anatomical structures of the carpal tunnel (carpal tunnel pressure), and as a result, compress upon the median nerve. Consequently, this mechanical deformation (also referred to as nerve entrapment) impairs the sensory and motor functions of the median nerve, eliciting CTS symptoms.

2. Literature Review

2.1) Carpal Tunnel Overview

The carpal tunnel of the wrist is a canal that is bordered on the dorsal aspect by the carpal bones, and on the palmar aspect by the transverse carpal ligament (TCL) (Figure 2.1.1). The TCL attaches radially on the scaphoid and trapezium bones, and ulnarly on the pisiform and hamate bones to enclose the tunnel (Figure 2.1.1). The 4 flexor digitorum superficialis (FDS) tendons, 4 flexor digitorum profundus (FDP) tendons, the flexor pollicis longus (FPL) tendon, and the median nerve (MN) pass from the distal forearm to the hand through the carpal tunnel (Figure 2.1.2). Geometrically, it has an area of approximately 180 mm² (Mogk & Keir, 2008), making it roughly 3/4th the size of a dime. Given the size of the carpal tunnel and the number of structures within, it is understandable why the median nerve may be compressed by an altered environment in the carpal tunnel.

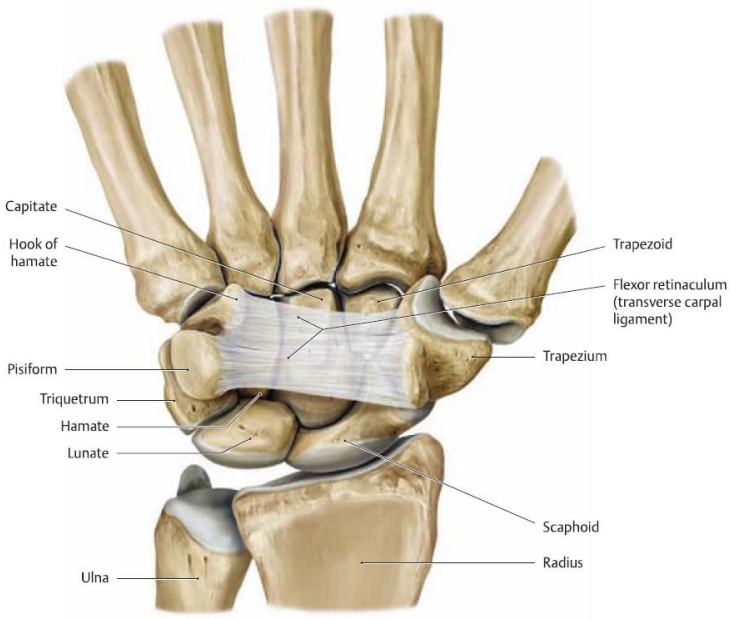

Figure 2.1.1. Boundaries of the carpal tunnel. Adapted from Schuenke et al. (2010).

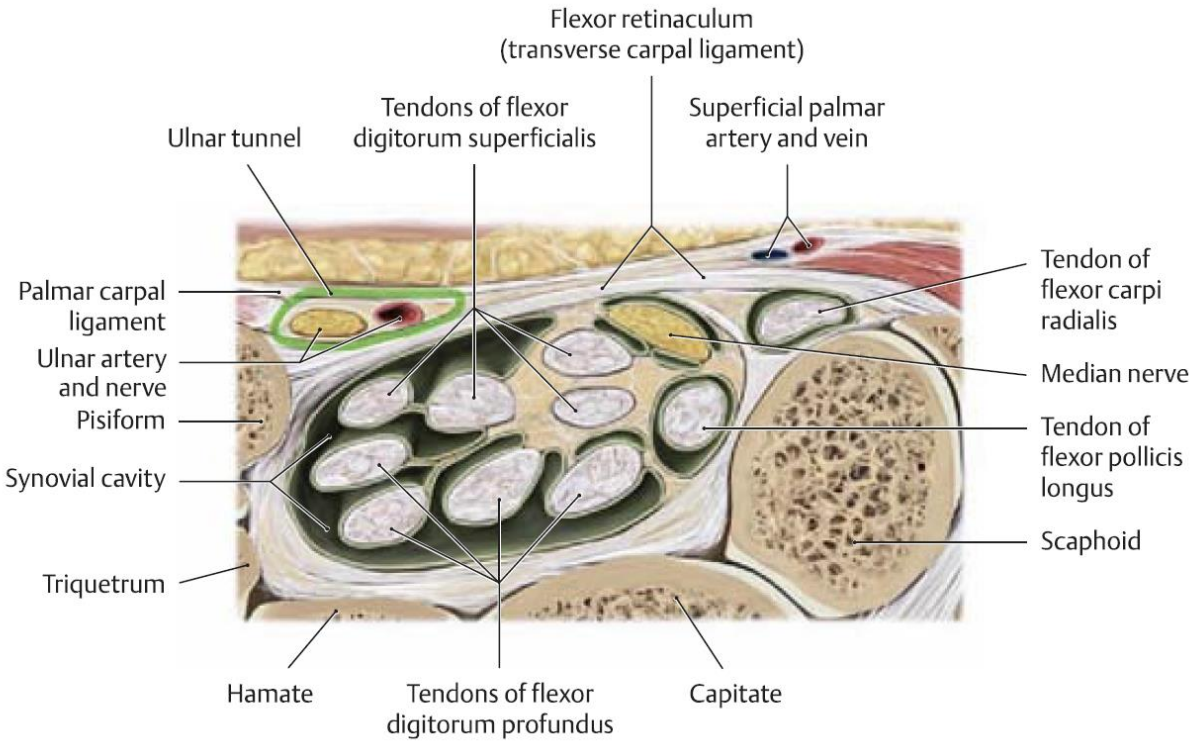

Figure 2.1.2. Cross section of the carpal tunnel and its contents. Adapted for clarity from Schuenke et al. (2010).

2.2) Carpal Tunnel Pressure

An elevation in carpal tunnel pressure (CTP) has long been associated to be a driving force for, or potential consequence of, carpal tunnel syndrome. Carpal tunnel pressure may be elevated by way of an increase in the volume of contents within the carpal tunnel, or a reduction in the volume of the carpal tunnel itself. The former may occur through muscle incursion into the carpal tunnel (Cobb, An, & Cooney, 1995; Keir & Bach, 2000), excess fluid within the tunnel, or enlargement of structures such as the median nerve. Alternatively, CTP is affected by alterations to the shape of the carpal tunnel through changes in finger and wrist joint angles, reducing the volume of the tunnel and increasing CTP. The established threshold for CTP that has been linked to CTS is

approximately 30 mmHg (Lundborg et al., 1982). With deviated wrist postures, CTP is elevated further. In CTS patients, wrist flexion increases CTP to about 94 mmHg, and extension to about 110 mmHg (Gelberman, Hergenroeder, Hargens, Lundborg, & Akeson, 1981). For cases in which no cause of CTS can be determined, referred to as "idiopathic" cases of CTS, CTP has been demonstrated to be lower: about 12 mmHg in a neutral wrist, 27 mmHg in a flexed wrist, and 33 mmHg in an extended wrist posture (Rojviroj et al., 1990). While individuals without CTS demonstrate a magnitude of CTP that falls below the critical threshold defined by Lundborg et al. (1982), the cumulative effects of factors such as wrist extension, radial deviation, and keyboard typing tasks may elevate CTP to 4 kPA, or 30 mmHg (Rempel, Keir, & Bach, 2008). Additionally, finger flexion has also been identified as a factor that influences CTP. CTP was found to be highest with metacarpophalangeal (MCP) joints in a neutral posture (0°), followed by MCP joints flexed to 90° and 45° (Keir, Bach, & Rempel, 1998). These findings hold true with wrist postures between 50° extension and 20° flexion. With further flexion, the effect of MCP angle on CTP was greatly diminished (Keir et al., 1998). The increase in CTP for patients with CTS is also non-uniform along the carpal tunnel, where the pressure is highest in the middle of the tunnel, and lower towards the inlet and outlet (Luchetti et al., 1989).

2.3) Subsynovial Connective Tissue

Surrounding the tendons and filling the space within the carpal tunnel is a structure known as the subsynovial connective tissue (SSCT). The SSCT consists of an intricate network of collagen bundles orientated in layers parallel to the tendons within

the carpal tunnel, with looser interconnecting fibres that join adjacent layers of the SSCT (Ettema et al., 2006; Guimberteau et al., 2010). The SSCT is viscoelastic with a gel-like consistency, with properties that can be attributed to its high water content and levels of proteoglycans and glycoaminoglycans (Guimberteau et al., 2010). As these compounds are negatively charged and draw in water (Guimberteau et al., 2010), it is plausible their hydrophilic property may extend to water retention in situations such as tissue edema.

As a microvacuolar system, the SSCT functions to alleviate shear stresses, lubricate structures, and provides a fluid environment within the carpal tunnel for structures of the cardiovascular, nervous, and lymphatic systems (Guimberteau et al., 2010). In cases of carpal tunnel syndrome, non-inflammatory fibrosis of the SSCT has been demonstrated to be the most common histological finding (Ettema et al., 2004; Ettema et al., 2006; Freeland et al., 2002; Jinrok et al., 2004; Neal et al., 1987). This is characterized by thickening of the parallel bundles of the SSCT and rupture of its interconnecting fibres (Ettema et al., 2006; Neal et al., 1987; van Doesburg et al., 2012). A mechanism that has been proposed to explain the pathophysiology of the SSCT and its relation to CTS is one of shear strain injury. In this injury mechanism, it is believed that excessive relative motion between the tendons in the carpal tunnel and its adjacent SSCT induces a cycle of rupture, repair, and thickening of the SSCT (Ettema et al., 2004). Using scanning electron microscopy on CTS patients, Ettema et al. (2006) found damage to the SSCT to be most prominent in the layers closest to the tendon, with superficial layers demonstrating less severe changes. The localization of SSCT damage suggests that a shearing injury may be the cause for pathological changes to the SSCT (Ettema et al.,

2006), and thus, relative tendon-SSCT motion may be best examined at this interface between the two structures to determine the effect of asynchronous tendon and SSCT motion on CTS pathology.

Understanding damage to the SSCT has been a topic of interest, particularly regarding progression and differences that exist between CTS and healthy populations. A noteworthy investigation conducted by Ettema et al. (2004) was in the form of histological analyses, where factors including collagen type, transforming growth factor-β, fibroblast density, and blood vessel abnormalities were examined. Higher levels of fibroblasts and collagen type III, as well as the presence of abnormal blood vessels and TGF-β, are indicators of soft tissue injuries. By extracting specimens of the SSCT from CTS patients undergoing surgery, and comparing these samples to those of healthy cadaver controls, evidence for an injury event to the pathological SSCT was believed to have occurred (Ettema et al., 2004). In the SSCT of CTS patients, fibroblasts, which play a pivotal role in wound repair and scar formation, were found at a higher count and density. In addition to the larger size of collagen fibers in CTS patients, the higher grading of collagen type III is also problematic, as it is weaker compared to collagen type I, and thus may facilitate further damage to the SSCT due to the lowered threshold for injury. Interestingly, TGF-β expression differences were found. Notably, these included 1) higher TGF-β RI in patients, and 2) the presence of TGF-β RII in endothelial cells only for healthy controls, compared to in the fibroblasts of the SSCT, endovascular smooth muscle, and endothelial cells for CTS patients. Combined, these histological changes provide evidence that the SSCT undergoes a healing process that is responsible for the

scarring and characteristic fibrosis found in the SSCT of CTS patients (Ettema et al., 2004).

Beyond the structural implications that impair the motion-related duties of the SSCT, results from the experiments conducted by Ettema et al. (2004) and Jinrok et al. (2004) support implications to vascular function as well. Interestingly, the vascular channels that permeate the SSCT were impacted, characterized by vascular proliferation, vascular hypertrophy, and vascular obstruction (Jinrok et al., 2004). Coupled with the higher expression of TGF-β in the smooth muscle and endothelial layers of the SSCT blood vessels (Ettema et al., 2004), it is clear that vascularity is affected in the pathological SSCT. Given excursion of finger flexor tendons has been demonstrated to result in mechanical deformation of SSCT blood vessels (Figure 2.3.1), it should be fair to assume that the shearing injury mechanism that causes fibrosis of the SSCT is responsible for these changes. The extent to which impaired SSCT vascular function impacts the median nerve, however, is less clear.

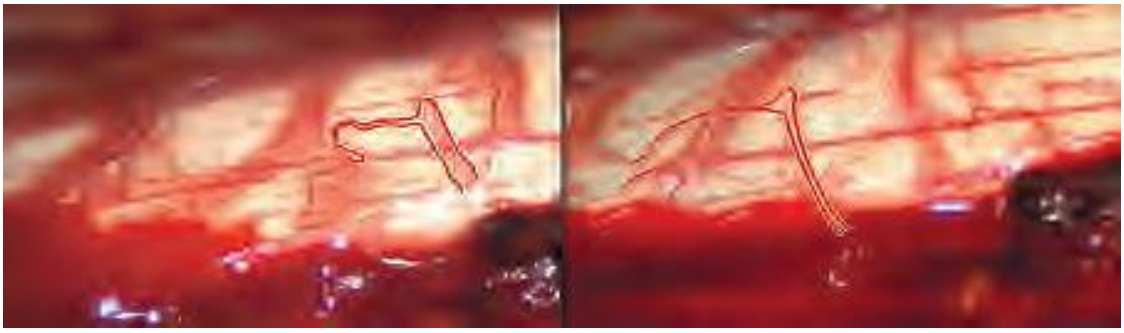

Figure 2.3.1. SSCT blood vessel with motion. (Left) Blood vessel of the SSCT at rest is outlined. (Right) Tendon excursion in the flexion direction, to the left, causes excursion of the blood vessel. (Adapted from Guimberteau, 2001).

2.4) Implications of Movement Speed on Carpal Tunnel Structures

Highly repetitive work has been associated with the development of occupational disorders, with ergonomic tools such as the Revised Strain Index (Garg, Moore, & Kapellusch, 2017) and American Conference of Governmental Industrial Hygienists Threshold Limit Value for Hand Activity (Yung et al., 2019) including repetition as a factor in their assessments of risk for developing injury. In the case of CTS, repetitive finger motion protocols have been performed to study the effect of repetitive work on parameters associated with the development of CTS. These investigations have taken the form of cadaveric studies, where the middle finger FDS tendon is isolated and moved using a motor (Kociolek, Tat, & Keir, 2015; Oh et al., 2007; Tat, Kociolek, & Keir, 2016, 2015), as well as in-vivo studies, where participants perform movements of the fingers or wrist and tissue motion is recorded using tools such as ultrasonography (Farias Zuniga, Ghavanini, Israelian, & Keir, 2020; Kociolek & Keir, 2016; Tat, Kociolek, & Keir, 2013; Tat, Wilson, & Keir, 2015; Tse & Keir, 2020).

With greater movement speed, tendon frictional work (a measure of resistance to gliding) due to differential finger motion increases, and is elevated further in a flexed wrist posture compared to neutral (Kociolek et al., 2015). Similarly, greater movement speed has also been linked to an increase in the Shear Strain Index (SSI) (Tat, Kociolek, et al., 2015). SSI is a metric that attempts to quantify the risk for injuring the SSCT. It is also important to note that this investigation found greater disparity between tendon excursion via operation by a motor, and ultrasound measured tendon displacement, demonstrating viscoelastic properties of the tendon at the tested movement speeds (Tat, Kociolek, et al.,

2015). Repetitive finger flexion is also affected by wrist posture, where wrist flexion increased the relative displacement index (identical to SSI) and decreased the maximum velocity ratio (MVR), implying more out of phase motion between the tendon and SSCT (Kociolek & Keir, 2016). Like SSI, MVR is a metric that quantifies the risk for injuring the SSCT; where SSI takes a displacement approach, MVR takes a velocity approach. Ultimately, the impact of movement speed of carpal tunnel structures on the potential for shear injury, may be due to significant decline in SSCT motion at higher velocities (Yoshii et al., 2011) compared to the finger flexor tendon, which is supported by the reduction in the ratio of SSCT velocity to tendon velocity at greater movement speeds (Oh et al., 2007).

2.5) Median Nerve

As a peripheral nerve, the median nerve has two distinct systems of vascularity: 1) the extrinsic system, which consists of vessels that originate from larger arteries and veins from the nerve's surroundings, and 2) the intrinsic system, which is made up of the plexuses of the epineurial, perineurial, and endoneurial layers of the nerve and their communicating vessels (Lundborg, 1975). Within the extrinsic system are coiled vessels that can accommodate large changes in nerve position before the vessels themselves are stretched and blood flow is impaired (Lundborg, 1975). Nerve function deteriorates within 30 to 90 minutes of ischemia, but quickly returns when blood flow is re-established (Lundborg, 1975), demonstrating the significant influence of blood flow restriction on the median nerve. This property may allow for interesting interactions with the SSCT regarding the shear injury mechanism of fibrosis. Given that the SSCT plays a role in

maintaining vascular continuity within the carpal tunnel, it aligns with the classification as a part of the extrinsic vascular system of the median nerve. In the healthy state, where the tendons and SSCT move coincident with one another, it can be posited that the vessels in the extrinsic system of the median nerve actually experience greater excursion compared to the pathological state, where relative motion between the tendon and SSCT is increased due to a reduction in SSCT displacement. Greater median nerve mobility in healthy individuals compared to those with CTS (Park et al., 2018) may further substantiate this claim, as the pathologically thickened SSCT may limit median nerve motion. Regardless, it is clear that further investigation must be made as to the exact vascular influence of the SSCT on the median nerve. Two mechanisms of impairment may be at play, where 1) the pathological SSCT impairs median nerve blood flow due to the thickened SSCT causing mechanical compression of the median nerve and its blood vessels, and 2) changes to the blood vessels of the SSCT could result in an increase in blood flow due to greater vascular proliferation (Jinrok et al., 2004) or alternatively, a reduction in blood flow as a result of altered vessel structure (Ettema et al., 2004; Jinrok et al., 2004) and consequently performance. With the latter, the influence of SSCT blood vessel alteration on median nerve blood flow may ultimately be tied to the state of CTS progression, where acute CTS may show greater median nerve blood flow from elevated SSCT blood flow driven by the repair process, while chronic CTS may show reduced median nerve blood flow due to limited influx from the SSCT as an extrinsic source of blood to the median nerve.

2.6) Median Nerve Blood Flow with CTS

As CTS is characterized by median nerve compression, one of the consequences is altered median nerve blood flow. Median nerve blood flow may differ based on the severity of symptoms, as undiagnosed individuals that present a greater number of symptoms—and thus, likelihood of CTS—have a higher median nerve blood flow velocity (13.3 cm/s) compared to those with fewer symptoms (8.5 cm/s) and healthy individuals (1.9 cm/s) (Joy, Therimadasamy, Chan, & Wilder-Smith, 2011). However, these patterns appear to be fairly complex, as another investigation on intraneural blood flow in symptomatic patients found flow to be lower in symptomatic patients (3.75 cm/s) compared to asymptomatic controls (4.27 cm/s) (Evans et al., 2012). Blood flow in the median nerve has also been demonstrated to be location dependent with respect to the carpal tunnel, with pulsatile flow proximal to the transverse carpal ligament, and random flow beneath it (Seiler et al., 1989). During this intra-operative investigation of median nerve blood flow during carpal tunnel release surgery, intraneural blood flow was found to change from random to pulsatile following surgery. This change was only detected at the segment of median nerve under the transverse carpal ligament; the segment proximal to this, however, was found to have pulsatile flow both before and after surgery. As a result, the authors believe this to be a sign that the segment of the median nerve trapped under the transverse carpal ligament is ischemic, and that this ischemia may be a factor in median nerve entrapment (Seiler et al., 1989). Related to the changes to blood flow pattern detected by Seiler et al. (1989), the magnitude of median nerve blood flow velocity was also found to increase following carpal tunnel release surgery (Soejima, Iida, & Naito,

2001). At the proximal and distal locations of the transverse carpal ligament, median nerve blood flow increased by 30% and 50%, respectively, although only the change to distal flow was found to be statistically significant (Soejima et al., 2001).

Similar changes have been demonstrated in an animal model of 12 rabbit sciatic nerves by Yayama et al. (2010), who tested the effect of mechanical compression of the nerve on intraneural blood flow. The compressive force applied at which intraneural blood flow stopped was similar to the magnitude that ceased action potential conduction in these nerves (0.457 and 0.486 N, respectively), demonstrating the integral role of blood flow on nerve function. Fluorescence microscopy was also used to evaluate the integrity of the blood-nerve barrier using Evans blue albumin. When intraneural ischemia was prolonged for 20 minutes, the presence of Evans blue albumin was found in nerve samples, suggesting a failure of the blood-nerve barrier. The authors believe their findings support an injury mechanism by which mechanical compression of a nerve leads to intraneural edema, demyelination of the nerve, ectopic discharge, and the onset of neuropathy. While these findings were derived from rabbit sciatic nerves, the underlying mechanism for neuropathy that connects nerve compression and entrapment, intraneural blood flow restriction, and edema to nerve damage may reasonably portray the sequence of events responsible for the development of carpal tunnel syndrome in human wrists.

Using contrast-enhanced ultrasonography, Motomiya et al. (2018) evaluated median nerve blood flow in CTS patients, providing a valuable link between SSCT and median nerve blood flow. Compared to healthy participants, those with CTS had higher blood flow in the SSCT prior to surgery. Additionally, after carpal tunnel release surgery,

the CTS patients had increased blood flow in both the median nerve and SSCT. Median nerve blood flow was found to significantly correlate with SSCT blood flow, and combined with the greater SSCT blood flow post-op, Motomiya et al. (2018) believe this to be evidence for the SSCT playing a role in altering the intraneural blood flow of the median nerve to support the nerve recovery process.

2.7) Biomechanical Influences on Median Nerve Blood Flow

Some of the recent literature investigating the relationship between SSCT (and consequently CTS) pathology and the median nerve has explored fluid and blood flow changes. In a cross-sectional investigation, Wilson et al. (2017) provided evidence of non-neutral wrist postures and fingertip forces increasing median nerve blood flow. Wrist postures deviated from 30° of flexion and extension, which are far more conservative than the 90° used in Phalen's test for CTS, yet a significant increase to median nerve blood flow velocity was detected with these wrist postures compared to a neutral wrist. Additionally, middle fingertip forces as low as 6 N elicited an increase to median nerve blood flow velocity, demonstrating how tasks with low force demands can contribute to median nerve blood flow changes. While patients that demonstrated symptoms for CTS generally had a higher median nerve blood flow velocity, the difference was not statistically significant (Wilson et al., 2017). When force application was extended to include various hand grips and wrist postures, main effects of grip and posture were also demonstrated (Ehmke et al., 2020). Irrespective of wrist posture, the application of force from the middle finger, thumb, or both increased median nerve blood flow velocity (Ehmke et al., 2020). Additionally, a 30° flexed wrist posture was found to have higher

blood flow velocity compared to neutral and extended wrist postures Ehmke (2020), while both flexed and extended wrist postures were found to significantly increase median nerve blood flow velocity compared to neutral in the findings by (Wilson et al., 2017). In fact, the 30° wrist extension posture actually resulted in a lower median nerve blood flow velocity compared to a neutral wrist in the cohort from Ehmke (2020). In terms of group differences, the findings by Ehmke (2020) mimic those of Wilson and colleagues (2017) where the CTS symptomatic participants showed elevated median nerve blood flow velocities compared to their healthy counterparts, albeit not statistically significant.

2.8) Considerations due to Biological Sex

Previously, it was believed that anthropometrics may contribute to the greater prevalence of CTS in females. Despite females having a smaller carpal tunnel compared to men, the size of the contents was not found to be different between males and females when normalized to the size of the carpal tunnel (Bower, Stanisz, & Keir, 2006). However, it is possible the viscoelastic nature of the SSCT may predispose females to a higher risk of developing CTS. Soft tissue edema is characteristic during periods of the female menstrual cycle (Tacani, de Oliveira Ribeiro, Guimarães, Machado, & Tacani, 2015) and pregnancy (Wilson & Allen, 2012). Edema within the SSCT, and by extension the carpal tunnel, would potentially result in elevated carpal tunnel pressure and compression of the median nerve. Functionally, the median nerve may also be implicated due to a deprivation of blood flow. With an altered fluid environment to the SSCT, the vascular supply that allows the median nerve to optimally perform its functions is impaired, leading to negative consequences in the form of CTS symptoms.

2.9) Altered Fluid and Median Nerve Blood Flow in the Carpal Tunnel

Fluid alteration has also been tested from an altered blood influx and efflux point of view. By inflating a blood pressure cuff on the upper arm of participants while performing repetitive finger motions, changes to finger flexor tendon and SSCT motion were detected (Tse & Keir, 2020; Wong et al., 2019). These findings support the potential link between pathological SSCT mechanics and CTS pathology. With blood pressure cuff inflation, the portion of the upper arm distal to the cuff—including the carpal tunnel—similarly has its pressure increased. With its blood flow impaired, median nerve function is quickly affected following the 30-90 minute time course indicated by Lundborg (1975). However, median nerve blood flow was not directly measured in the studies performed by Tse & Keir (2020) and Wong et al. (2019), and thus the mechanism by which changes took place can only be theorized. On one hand, the supradiastolic pressure (condition termed "partial ischemia", between diastolic blood pressure (DBP) and systolic blood pressure (SBP)) utilized by Tse & Keir (2020) would most likely have impacted median nerve blood flow in two ways. The first is that the use of a supradiastolic pressure from brachial blood pressure cuff inflation limited blood influx to the nerve, causing a bottleneck effect to limit nerve function. However, the second way median nerve blood flow is impacted is that the same supradiastolic pressure, being higher than venous pressure, prevents blood efflux from the distal upper extremity. Effectively, this creates a situation where fluid retention may take place in the carpal tunnel, leading to tissue edema that reduces median nerve blood flow due to mechanical compression of the median nerve from the greater volume of contents in its surroundings. To investigate

this, a follow up study was performed by Wong et al. (2019) where brachial cuff inflation was applied at a subdiastolic pressure (condition termed "occlusion") to experimentally induce the tissue edema condition. Similarly, changes to SSCT motion were detected, with the subdiastolic pressure used in the occlusion condition decreasing SSCT displacement irrespective of finger movement speed. This provides evidence in support of edema being the driving factor in altered local blood flow, as the lower pressure of occlusion tested in Wong et al. (2019) should not inhibit blood efflux from the hand and wrist, unlike the higher pressure in partial ischemia (Tse & Keir, 2020). However, it is certainly important to note that more investigation is needed in this area, as these studies only had samples of 20 healthy young participants each. Whether these findings extend to older populations, are demonstrated in individuals with conditions that may alter the fluid environment in the carpal tunnel, or are applicable to CTS patients is yet to be determined.

3. Purpose

This investigation aims to evaluate findings from various studies in the McMaster Occupational Biomechanics Laboratory and summarize changes to median nerve blood flow and tendon/SSCT motion. Of key interest is to evaluate the effect of biomechanical factors on these outcomes, how these outcomes influence one another, and provide a holistic picture of the mechanism relating these outcomes to the progression of CTS.

4. Hypotheses

1) An inverse relationship exists between movement speed and displacement of the finger flexor tendon and SSCT. As movement speed increases, displacement decreases. This is driven by the reduction in viscoelastic strain at higher movement speeds.
2) Median nerve blood flow velocity is greater:
    i. in non-neutral wrist postures.
    ii. with force application.
    iii. with CTS, compared to symptomatic and healthy subjects.
3) Fluid/blood flow alteration in the carpal tunnel:
    i. disproportionately affects the movement of the SSCT compared to the FDS tendon.
    ii. is comparable to people with CTS, when applied to healthy subjects.

5. Methods

Separate analyses were performed to elucidate different aspects of finger motion, wrist posture, median nerve blood flow, and population sample in relation to CTS pathology. Significance was defined at $p < 0.05$. Studies that were considered for inclusion were conducted in the McMaster Occupational Biomechanics Lab and are listed in Appendix 1.

5.1) Biomechanical Influences on Tendon and SSCT Motion

Data from a total of 128 subjects (76 healthy, 33 CTS, 11 symptomatic patents, 8 cadaveric) were analyzed from 7 studies to assess the effects of finger movement speed and wrist posture on ultrasound measured tendon and SSCT motion. The list of studies is as follows: Farias Zuniga et al. (2020), referred to as AFZ1; Farias Zuniga (2020), referred to as AFZ2; Kociolek & Keir (2016), referred to as Kociolek (2016); (Tat, Wilson, & Keir, 2015), referred to as Tat (2015a); Tat et al. (2016), referred to as Tat (2016); Tse & Keir (2020), referred to as Tse (2020); Wong et al. (2019), referred to as Wong (2019). The dataset for this group of investigations is detailed in Table 5.1.

Table 5.1. Sample and analysis details for investigation of biomechanical influences on tendon and SSCT motion. Wrist postures (N = Neutral, Fl = Flexion, Ex = Extension), subjects, and observations in each included cohort are provided. Analysis involved using the predictors of FDS velocity, SSCT velocity, and wrist posture to predict the outcomes of FDS displacement, SSCT displacement, relative displacement, SSI, and MVR.

Sample				**Analysis**	
Study	**Wrist Postures**	**Subjects**	**Observations**	**Predictors**	**Outcomes**
AFZ1	N	33	49	FDS velocity SSCT velocity Wrist Posture	FDS Displacement SSCT Displacement Relative Displacement SSI MVR
AFZ2	N	10	47		
Kociolek (2016)	Ex, N, Fl	16	48		
Tat (2015a)	N	22	22		
Tat (2016)	N, Fl	8	144		
Tse (2020)	N	19	190		
Wong (2019)	N	20	80		

5.1.1) Finger Movement Speed

Individual studies from the dataset outlined in Table 5.1 included protocols involving repetitive finger flexion and extension cycles at various frequencies and speeds: from 0.75 Hz (Farias Zuniga et al., 2020; Tse & Keir, 2020; Wong et al., 2019), 1 Hz (Tat, Wilson, & Keir, 2015), 1.25 Hz (Tse & Keir, 2020; Wong et al., 2019), a self-selected pace corresponding to approximately 60 mm/s tendon velocity (Kociolek & Keir, 2016), and cadaveric tendon excursion velocities of 50-150 mm/s (Tat et al., 2016). For any studies that separated finger motion into its flexion and extension phases, average values were calculated for the data. Average trial velocities and wrist posture from the dataset were analyzed in a mixed effects model, with 1) mean peak FDS tendon displacement, 2) mean peak SSCT displacement, and 3) strain measures (relative tendon-SSCT displacement, SSI, and MVR) as outcome variables.

5.1.2) Deviated Wrist Postures

From the total dataset, studies that conducted finger motion in multiple wrist postures include the Kociolek & Keir (2016) study (extension, neutral, and flexion), and the Tat et al. (2016) study (neutral and flexion). Despite mixing data from in-vivo and ex-vivo sources, the cadaveric samples (Tat et al., 2016) underwent a protocol involving 30 mm of tendon excursion, with 20 mm of the middle range being analyzed. This makes a comparison possible due to falling within physiological ranges as well as similarity to values obtained by Kociolek & Keir (2016). Trials from the Kociolek & Keir (2016) cohort were collapsed across all finger movement types (MCP, PIP + DIP, and full finger) due to the lack of statistical differences determined in the study. Wrist posture was treated

as a predictor with three distinct levels (Extension, Neutral, and Flexion). Mixed effects models assessed the effect of wrist posture on displacements (FDS tendon and SSCT) and strain measures (relative tendon-SSCT displacement, SSI, and MVR).

5.2) Median Nerve Blood Flow Changes

5.2.1) Biomechanical Influences on Median Nerve Blood Flow

Participants from the Wilson, Tat, & Keir (2017), Ehmke (2020), Farias Zuniga et al. (2020), and Farias Zuniga (2020) cohorts were pooled to determine the overall effect of finger force and deviated wrist postures on median nerve blood flow. Subjects that were undiagnosed but experienced CTS symptoms were grouped as "possible" for CTS status. A total sample size of 109 participants were included for analysis (Table 5.2). Wrist postures were grouped into three levels (extension, neutral, and flexion). Mixed effects models assessed the effects of wrist posture, force (0 N, 6 N middle finger), and the interaction effect of wrist posture × force on median nerve blood flow.

Table 5.2. Sample and analysis details for investigation of biomechanical influences on median nerve blood flow velocity (BFV). The number of wrist postures (extension, neutral, flexion), forces (0 N, 6 N), subjects, and observations in each included cohort are provided. Analysis involved using the predictors of wrist posture and force to predict median nerve BFV.

	Sample				Analysis	
Study	**Wrist Postures**	**Forces**	**Subjects**	**Observations**	**Predictors**	**Outcomes**
AFZ1	Ex, N, Fl	1	33	126	Wrist Posture Force	Median Nerve BFV
AFZ2	N	1	36	176		
Ehmke (2020)	Ex, N, Fl	2	22	330		
Wilson (2017)	Ex, N, Fl	2	18	180		

5.2.2) Group Differences

An analysis of the effect of CTS status on median nerve blood flow included data from 56 healthy (Ehmke et al., 2020; Wilson, Tat, & Keir, 2017), 20 possible (Ehmke et al., 2020; Wilson, Tat, & Keir, 2017), 32 CTS (Farias Zuniga et al., 2020), and 16 follow-up subjects (Farias Zuniga et al., 2020) (Table 5.3). The influence of CTS status and presence of symptoms was assessed in three models to test the effect of classification on median nerve blood flow velocity (Table 5.4). CTS status was tested with levels of 1) Healthy, 2) Possible, 3) CTS, and 4) Follow-Up with mean peak blood flow velocity as the outcome. A second model with CTS categorized into its respective severities was tested, with CTS status broken up into levels 1) Healthy, 2) Possible, 3) Mild, 4) Moderate, 5) Severe, 6) Follow-Up. Finally, median nerve blood flow was compared between groups by the presence of symptoms, with healthy subjects in the "No" group, and possible, CTS, and follow-up subjects in the "Yes" group.

Table 5.3. Sample and analysis details for investigation of CTS status on median nerve blood flow velocity (BFV). The number of CTS statuses (healthy, possible, CTS, follow-up), severities (healthy, possible, mild, moderate, severe, follow-up), symptoms (yes, no), subjects, and observations in each included cohort are provided. Analysis involved using the predictor of CTS status to predict median nerve BFV.

	Sample					Analysis	
Study	**CTS Statuses**	**Severities**	**Symptoms**	**Subjects**	**Observations**	**Predictors**	**Outcomes**
AFZ1	2	4	2	33	126	CTS Status	Median Nerve BFV
AFZ2	1	1	1	36	176		
Ehmke (2020)	2	2	2	22	330		
Wilson (2017)	2	2	2	18	180		

Table 5.4. Breakdown of CTS status levels used to predict median nerve blood flow for each model. Model #1 classifies CTS status into 4 levels (healthy, possible, CTS, follow-up). Model #2 incorporates CTS severities and results in 6 total levels (healthy, possible, mild, moderate, severe, follow-up). Model #3 uses the presence of symptoms only (yes, no), where the follow-up group is included in the yes symptom group. Subjects and observations in each included model are provided.

	CTS Status	**Subjects**	**Observations**
Model #1	Healthy	56	431
	Possible	20	255
	CTS	32	89
	Follow-Up	16	37
Model #2 (Severities)	Healthy	56	431
	Possible	20	255
	Mild	11	32
	Moderate	13	33
	Severe	8	24
	Follow-Up	16	37
Model #3 (Symptoms)	Symptoms	56	431
	No Symptoms	53	381

5.3) Effect of Induced Blood Flow Alteration

5.3.1) Tendon and SSCT Motion

Data from 49 participants were pooled from the Tse & Keir (2020) and Wong et al. (2019) cohorts. Repetitive differential motion of the middle finger was analysed to determine the net effect of 1) altered local blood flow in the carpal tunnel (yes vs no), and 2) the type of blood flow alteration (baseline vs subdiastolic vs supradiastolic) on displacements and strain measures. Aside from the pressure for local blood flow alteration, collection and processing procedures were essentially identical amongst the studies. To elicit altered blood flow, a manual blood pressure cuff was inflated and held at a constant pressure on the upper arm. Tse & Keir (2020) used DBP + 0.25(SBP-DBP) in a supradiastolic condition (termed by authors as partial ischemia using subsystolic pressure), whereas Wong, Farias Zuniga, & Keir (2019) and Farias Zuniga (2020) restricted blood flow using 0.8 × DBP in a subdiastolic condition. Sample and analysis details are outlined in Table 5.5.

Table 5.5. Sample and analysis details for investigation of local blood flow alteration on tendon and SSCT motion. The type of blood flow alteration used (subdiastolic, supradiastolic), subjects, and observations in each included cohort are provided. Analysis involved using the predictor of altered blood flow on displacements (FDS, SSCT), and strain measures (relative displacement, SSI, MVR).

Sample				Analysis	
Study	**Altered Blood Flow**	**Subjects**	**Observations**	**Predictors**	**Outcomes**
AFZ2	Subdiastolic	10	176	Altered BF	Displacement (FDS, SSCT, Relative)
Tse (2020)	Supradiastolic	19	330	Altered BF Type	SSI
Wong (2019)	Subdiastolic	20	180		MVR

5.3.2) CTS Comparison

Data from investigations 5.2.2 (Table 5.3) and 5.3.1 (Table 5.5) were consolidated to infer whether induced blood flow alteration in an experimental setting is comparable to behaviour exhibited by individuals with CTS. Local blood flow alteration performed by Farias Zuniga (2020) in healthy subjects was compared to median nerve blood flow in subjects with varying CTS status (healthy, possible, mild, moderate, severe, and follow-up) to establish the group(s) sharing the greatest similarity. CTS status was used in a mixed effects model to predict median nerve blood flow velocity. Only observations with a neutral wrist posture and no force generation were used for this comparison.

Table 5.6. Breakdown of CTS status levels used to predict median nerve blood. Healthy-T1 to Healthy-T4 represent healthy subjects in the AFZ2 cohort with induced local blood flow alteration. Note that there exists overlap amongst the healthy statuses due to the nature of eliciting altered local blood flow. Observations are taken in a neutral wrist posture with 0 N force.

	CTS Status	Subjects	Observations
Altered Blood Flow & CTS Comparison	Healthy	56	67
	Healthy-T1	35	35
	Healthy-T2	35	35
	Healthy-T3	34	32
	Healthy-T4	36	36
	Possible	20	31
	Mild	10	10
	Moderate	12	12
	Severe	8	8
	Follow-Up	12	12

5.4) Statistics

Analysis was conducted using R (R Core Team, 2021). The lmerTest package (Kuznetsova, Brockhoff, & Christensen, 2017) was used to generate linear mixed effects models and determine the effects of the predictors on the outcomes of interest. Regression assumptions were visually assessed. Models were created with subject nested within study, and both subject and study were included into the model as random effects. Variance of the model is represented by conditional R^2, defined as the total variance explained by both the fixed and random effects in the model (Nakagawa & Schielzeth, 2013).

6. Results

6.1) Biomechanical Influences on Tendon and SSCT Motion

6.1.1) FDS Displacement

FDS tendon velocity was demonstrated to significantly predict FDS tendon displacement (Figure 6.1a). The regression model explained 80.4% of the variance, with velocity contributing significantly to the model ($\beta = -0.013$, $p < 0.01$). Wrist posture was also found to significantly predict FDS tendon displacement, where wrist flexion, but not extension, was found to reduce the extent of displacement ($\beta = -0.133$, $p < 0.01$) compared to a neutral wrist posture (Figure 6.1b). All regression results are reported in Table 6.1.

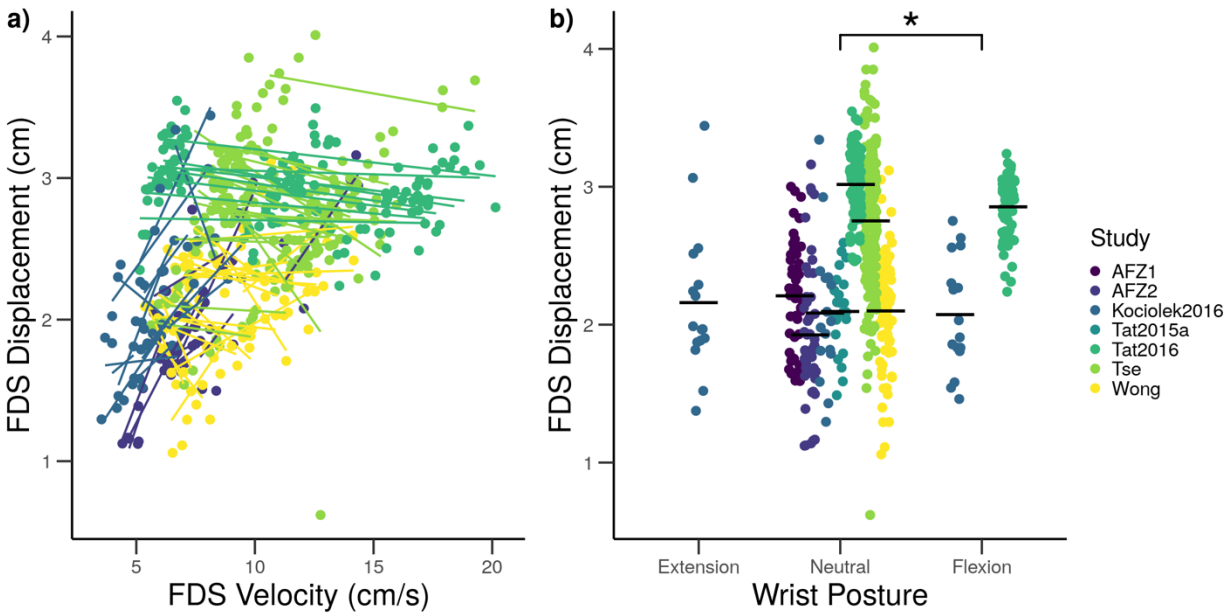

Figure 6.1. FDS Displacement results for velocity and wrist posture. a) Velocity and displacement of the FDS tendon with lines of best fit for each subject. Model results indicate a decrease in displacement with increasing velocity. b) FDS displacement at varying wrist postures. Horizontal bars represent the mean value from a study in the given wrist posture. Wrist flexion was found to decrease FDS displacement compared to the neutral position.

Table 6.1. Model results for FDS and SSCT displacements. Estimates represent the beta-coefficient for the associated predictor variable and are provided with 95% confidence intervals (CI). Significant results are bolded and defined at a level of $p < 0.05$. The intercept represents the estimate for the reference group, and are the following for the predictor variables: FDS Velocity, 0 cm/s; Wrist Posture, Neutral; SSCT Velocity, 0 cm/s. The between group variance for the random effects are provided in the rows denoted by τ_{00}. Where applicable, individual study results from each model are detailed in Appendix 2.1 and Appendix 2.2.

	FDS Displacement			**FDS Displacement**			**SSCT Displacement**			**SSCT Displacement (Outliers Removed)**			**SSCT Displacement**		
Predictors	*Estimates*	*CI*	*p*	*Estimates*	*CI*	*p*	*Estimates*	*CI*	*p*	*Estimates*	*CI*	*p*	*Estimates*	*CI*	*p*
(Intercept)	2.48	2.05 – 2.90	**<0.001**	2.32	2.02 – 2.61	**<0.001**	2.04	1.66 – 2.43	**<0.001**	2.13	1.72 – 2.55	**<0.001**	1.90	1.64 – 2.16	**<0.001**
FDS Velocity	-0.01	-0.02 – -0.00	**0.004**												
Wrist Posture (Flexion)				-0.13	-0.22 – -0.05	**0.002**							-0.29	-0.39 – -0.19	**<0.001**
Wrist Posture (Extension)				0.01	-0.16 – 0.19	0.881							0.11	-0.10 – 0.31	0.321
SSCT Velocity							-0.01	-0.03 – 0.00	0.096	-0.03	-0.05 – -0.01	**<0.001**			
Random Effects															
σ^2	0.08			0.08			0.13			0.10			0.12		
τ_{00}	0.11 $_{\text{Subject:Study}}$			0.09 $_{\text{Subject:Study}}$			0.10 $_{\text{Subject:Study}}$			0.10 $_{\text{Subject:Study}}$			0.08 $_{\text{Subject:Study}}$		
	0.22 $_{\text{Study}}$			0.15 $_{\text{Study}}$			0.17 $_{\text{Study}}$			0.20 $_{\text{Study}}$			0.12 $_{\text{Study}}$		
N	73 $_{\text{Subject}}$			128 $_{\text{Subject}}$			73 $_{\text{Subject}}$			72 $_{\text{Subject}}$			128 $_{\text{Subject}}$		
	5 $_{\text{Study}}$			7 $_{\text{Study}}$			5 $_{\text{Study}}$			5 $_{\text{Study}}$			7 $_{\text{Study}}$		
Observations	509			580			509			497			580		
Marginal R^2 / Conditional R^2	0.005 / 0.804			0.007 / 0.746			0.004 / 0.680			0.014 / 0.746			0.035 / 0.645		

6.1.2) SSCT Displacement

Wrist posture was found to significantly predict SSCT displacement ($R^2 = 0.645$) (Figure 6.2b). Compared to the wrist in a neutral posture, wrist flexion was found to reduce SSCT displacement ($\beta = -0.291$, $p < 0.001$). SSCT velocity was not found to significantly predict SSCT displacement ($\beta = -0.015$, $p = 0.096$) (Figure 6.2a). Upon removal of outliers identified using Cook's distance, SSCT velocity was found to significantly predict SSCT displacement ($\beta = -0.030$, $p < 0.001$) with the model explaining 74.6% of the variance ($R^2 = 0.746$). Regression model results are reported in Table 6.1.

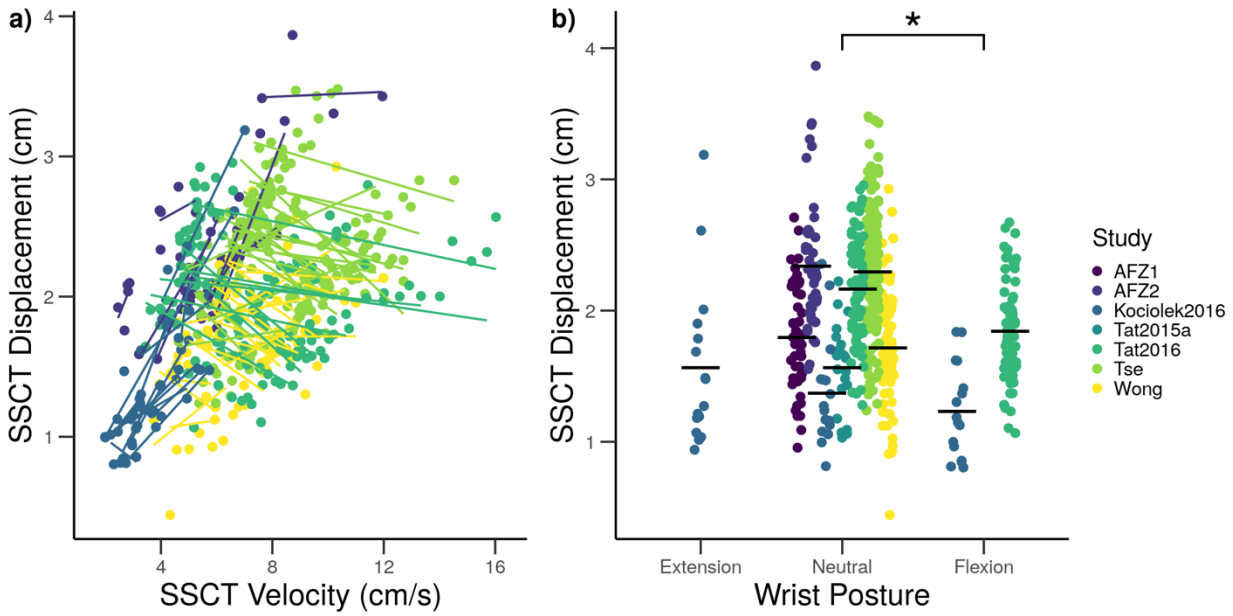

Figure 6.2. SSCT Displacement results for velocity and wrist posture. a) Velocity and displacement of the SSCT tendon with lines of best fit for each subject. Model results indicate a decrease in displacement with increasing velocity only after removal of outliers. b) SSCT displacement at varying wrist postures. Horizontal bars represent the mean value from a study in the given wrist posture. Wrist flexion was found to decrease SSCT displacement compared to the neutral position.

6.1.3) Strain Measures

FDS velocity was found to significantly predict relative displacement ($\beta = 0.035$, $p < 0.001$), shear strain index (SSI) ($\beta = 1.398$, $p < 0.001$), and maximum velocity ratio (MVR) ($\beta = -1.933$, $p < 0.001$). As FDS velocity increases, both the relative displacement and SSI increase, while MVR decreases (Figure 6.3). SSCT velocity was not found to predict relative displacement ($\beta = -0.006$, $p = 0.409$), SSI ($\beta = 0.132$, $p = 0.575$), or MVR ($\beta = -0.437$, $p = 0.078$). Upon removal of outliers identified via Cook's distance, SSCT velocity was found to significantly predict MVR ($\beta = -0.793$, $p < 0.001$). All regression results are reported in Table 6.2.

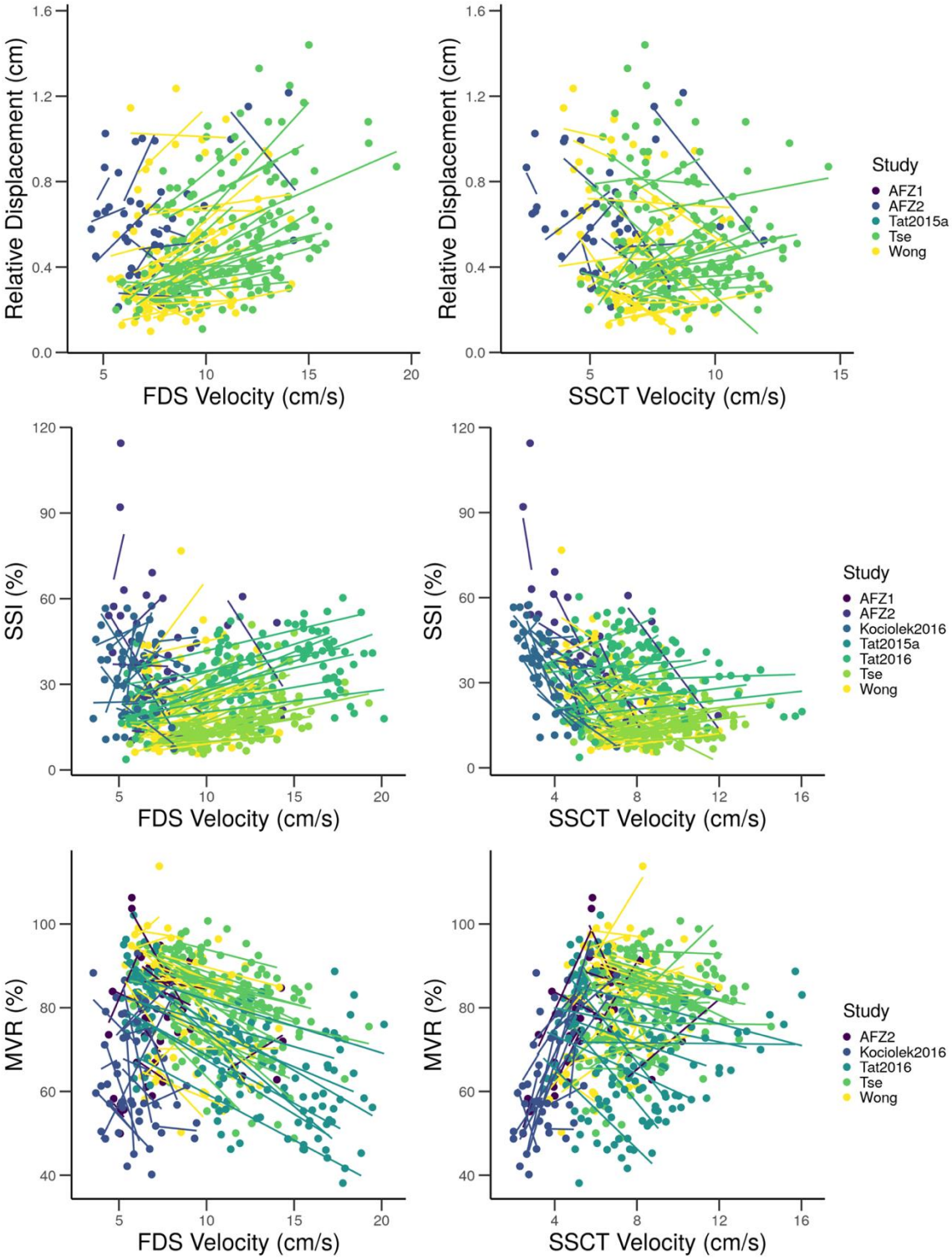

Figure 6.3. Strain measures by FDS velocity (left) and SSCT velocity (right). Rows represent data for relative displacement, SSI, and MVR, respectively.

Table 6.2. Model results for shear measures (relative displacement, SSI, and MVR). Estimates represent the beta-coefficient for the associated predictor variable and are provided with 95% confidence intervals (CI). Significant results are bolded and defined at a level of $p < 0.05$. The intercept represents the estimate for the reference group, and are the following for the predictor variables: FDS Velocity, 0 cm/s; SSCT Velocity, 0 cm/s. The between group variance for the random effects are provided in the rows denoted by τ_{00}. Where applicable, individual study results from each model are detailed in Appendix 2.3 – Appendix 2.10.

	Relative Displacement			**Relative Displacement**			**SSI**			**SSI**			**MVR**			**MVR**			**MVR (Outliers Removed)**		
Predictors	*Estimates*	*CI*	*p*	*Estimates*	*CI*	*p*	*Estimates*	*CI*	*p*	*Estimates*	*CI*	*p*	*Estimates*	*CI*	*p*	*Estimates*	*CI*	*p*	*Estimates*	*CI*	*p*
(Intercept)	0.20	0.05 – 0.35	**0.010**	0.54	0.43 – 0.66	**<0.001**	16.16	6.45 – 25.88	**0.001**	27.60	19.18 – 36.01	**<0.001**	92.08	83.02 – 101.15	**<0.001**	77.87	70.05 – 85.70	**<0.001**	79.92	71.64 – 88.20	**<0.001**
FDS Velocity	0.03	0.03 – 0.04	**<0.001**				1.40	1.14 – 1.66	**<0.001**				-1.93	-2.18 – -1.68	**<0.001**						
SSCT Velocity				-0.01	-0.02 – 0.01	0.409				0.13	-0.33 – 0.59	0.574				-0.44	-0.92 – 0.05	0.078	-0.79	-1.25 – -0.34	**0.001**
Random Effects																					
σ^2	0.03			0.03			66.75			84.66			63.34			95.43			80.88		
τ_{00}	0.04 Subject:Study			0.04 Subject:Study			100.30 Subject:Study			92.01 Subject:Study			74.54 Subject:Study			73.26 Subject:Study			85.20 Subject:Study		
	0.01 Study			0.00 Study			107.45 Study			72.07 Study			94.00 Study			59.66 Study			69.80 Study		
N	49 Subject			49 Subject			73 Subject			73 Subject			73 Subject			73 Subject			73 Subject		
	3 Study			3 Study			5 Study			5 Study			5 Study			5 Study			5 Study		
Observations	317			317			509			509			509			509			495		
Marginal R^2 / Conditional R^2	0.115 / 0.673			0.002 / 0.554			0.080 / 0.776			0.000 / 0.660			0.165 / 0.772			0.005 / 0.584			0.016 / 0.663		

6.2 Median Nerve Blood Flow Changes

6.2.1) Biomechanical Influences on Median Nerve Blood Flow

Force ($\beta = 0.583$, $p < 0.001$) and wrist posture ($\beta = 0.243$, $p = 0.01$) were found to influence median nerve blood flow velocity. Specifically, wrist flexion and 6 N of force generation were associated with greater median nerve blood flow velocities (Figure 6.4). Regression results for the effects of wrist posture and force application on median nerve blood flow velocity are reported in Table 6.3.

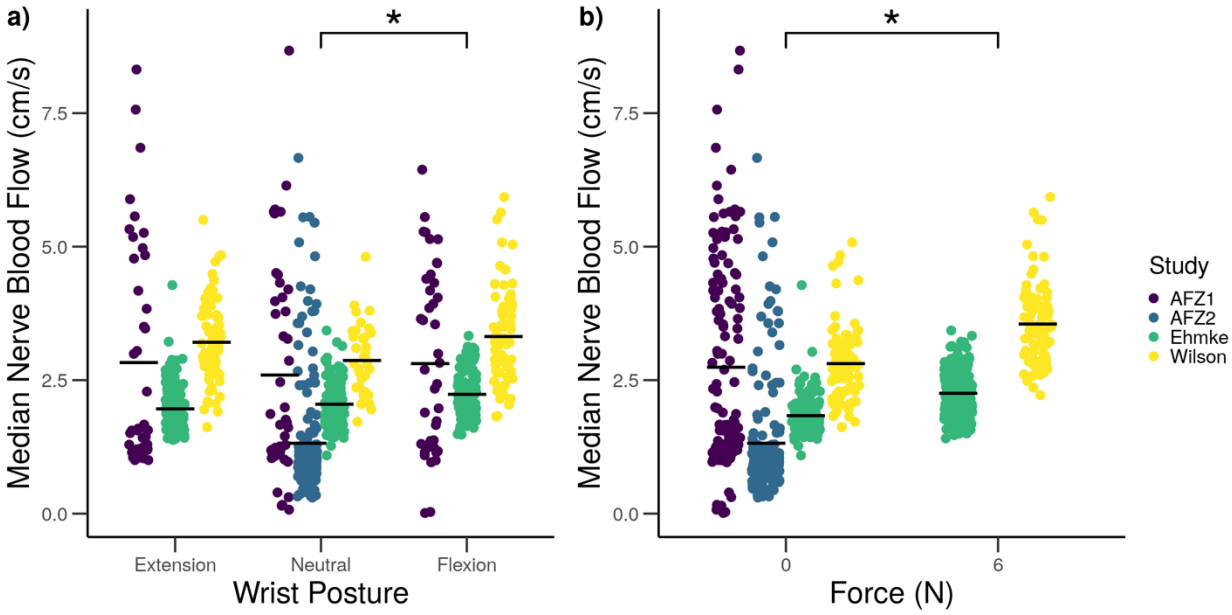

Figure 6.4. Median nerve blood flow velocity by a) wrist posture and b) force. a) In a flexed wrist posture, median nerve blood flow is greater compared to a neutral wrist. b) With the generation of 6 N of finger force, median nerve blood flow is greater compared to no finger force. Horizontal black bars represent group means.

Table 6.3. Model results for median nerve (MN) blood flow velocity (BFV). Estimates represent the beta-coefficient for the associated predictor variable and are provided with 95% confidence intervals (CI). Significant results are bolded and defined at a level of $p < 0.05$. The intercept represents the estimate for the reference group, and are the following for the predictor variables: Wrist Posture, Neutral; Force, 0 N. The between group variance for the random effects are provided in the rows denoted by τ_{00}.

	Median Nerve BFV			**Ehmke**			**Wilson**		
Predictors	*Estimates*	*CI*	*p*	*Estimates*	*CI*	*p*	*Estimates*	*CI*	*p*
(Intercept)	2.08	1.37 – 2.79	**<0.001**	1.77	1.64 – 1.90	**<0.001**	2.50	2.17 – 2.83	**<0.001**
Wrist Posture (Flexion)	0.24	0.06 – 0.43	**0.011**	0.24	0.09 – 0.39	**0.002**	0.40	0.03 – 0.76	**0.034**
Wrist Posture (Extension)	0.15	-0.04 – 0.33	0.119	-0.03	-0.18 – 0.12	0.695	0.39	0.02 – 0.76	**0.037**
Force (6 N)	0.58	0.37 – 0.80	**<0.001**	0.48	0.34 – 0.61	**<0.001**	0.75	0.33 – 1.17	**0.001**
Wrist Posture × Force (Flexion × 6 N)	0.01	-0.26 – 0.29	0.925	-0.08	-0.28 – 0.11	0.395	0.10	-0.42 – 0.61	0.715
Wrist Posture × Force (Extension × 6 N)	-0.15	-0.42 – 0.13	0.296	-0.10	-0.29 – 0.10	0.334	-0.11	-0.63 – 0.41	0.685
Random Effects									
σ^2	0.50			0.13			0.42		
τ_{00}	0.96 $_{\text{Subject:Study}}$ 0.48 $_{\text{Study}}$			0.03 $_{\text{Subject}}$			0.09 $_{\text{Subject}}$		
ICC	0.74			0.18			0.17		
N	109 $_{\text{Subject}}$ 4 $_{\text{Study}}$			22 $_{\text{Subject}}$			18 $_{\text{Subject}}$		
Observations	812			330			180		
Marginal R^2/ Conditional R^2	0.045 / 0.755			0.259 / 0.389			0.250 / 0.378		

5.2.2) Group Differences

When CTS status was categorized with the levels 1) Healthy, 2) Possible, 3) CTS, and 4) Follow-Up (Figure 6.5), differences were only detected between the CTS and Follow-Up groups ($\beta = -0.600$, $p < 0.001$) (Appendix 3.3). After separating the CTS group into its respective severities (Mild, Moderate, and Severe) (Figure 6.5), differences were detected between the Mild and Severe groups ($\beta = 0.832$, $p < 0.05$), Moderate and Follow-Up groups ($\beta = -0.614$, $p < 0.01$), and Severe and Follow-Up groups ($\beta = -1.172$, $p < 0.001$) (Appendix 3.5). Finally, median nerve blood flow was not found to be significantly predicted by the presence of CTS symptoms ($\beta = 0.318$, $p = 0.29$) (Table 6.4).

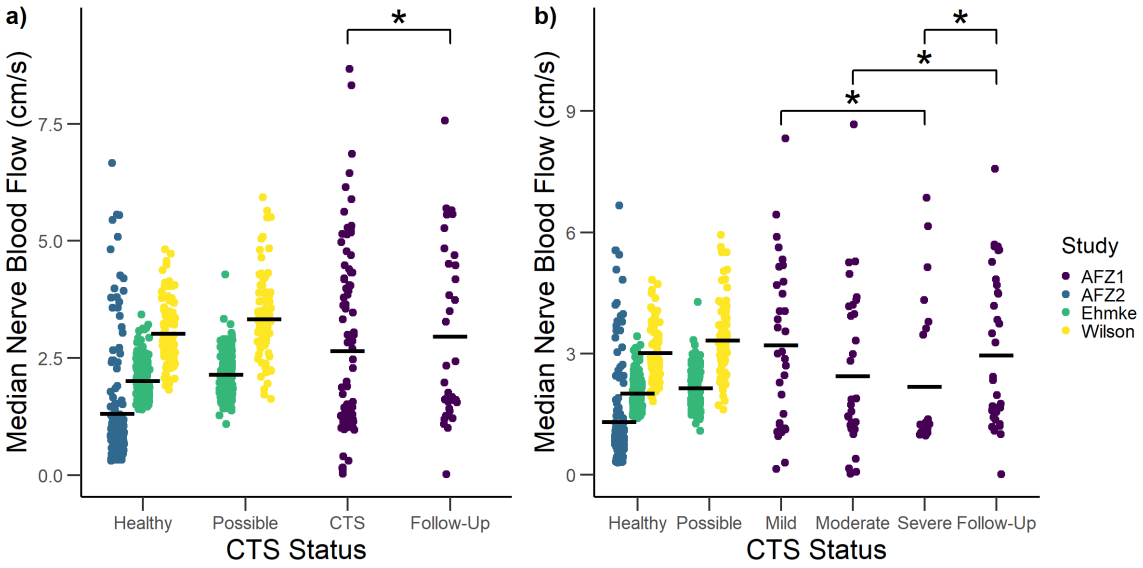

Figure 6.5. Median nerve blood flow velocity by CTS status. Group means are represented by horizontal black bars. a) Difference detected between CTS and Follow-Up groups. b) CTS group split into severities. Differences are present between Mild and Severe groups, Moderate and Follow-Up groups, and Severe and Follow-Up groups.

Table 6.4. Model results for median nerve blood flow velocity (BFV) with CTS Status, CTS Status 2 (where CTS is separated into its severities), and Symptoms as predictors. Estimates represent the beta-coefficient for the associated predictor variable and are provided with 95% confidence intervals (CI). Significant results are bolded and defined at a level of $p < 0.05$. The intercept represents the estimate for the reference group (CTS Status = Healthy; CTS Status 2 = Healthy; Symptoms = No). The between group variance for the random effects are provided in the rows denoted by τ_{00}. Where applicable, individual study results from each model are detailed in Appendix 3.2 – Appendix 3.6.

	Median Nerve BFV			**Median Nerve BFV**			**Median Nerve BFV**		
Predictors	*Estimates*	*CI*	*p*	*Estimates*	*CI*	*p*	*Estimates*	*CI*	*p*
(Intercept)	2.10	1.08 – 3.12	**<0.001**	2.10	1.08 – 3.12	**<0.001**	2.17	1.39 – 2.95	**<0.001**
CTS Status (Possible)	0.27	-0.35 – 0.88	0.398						
CTS Status (CTS)	0.51	-1.49 – 2.50	0.620						
CTS Status (Follow-Up)	1.11	-0.91 – 3.12	0.281						
CTS Status 2 (Possible)				0.27	-0.35 – 0.88	0.396			
CTS Status 2 (Mild)				0.82	-1.21 – 2.86	0.426			
CTS Status 2 (Moderate)				0.55	-1.48 – 2.58	0.595			
CTS Status 2 (Severe)				-0.01	-2.07 – 2.05	0.994			
CTS Status 2 (Follow-Up)				1.16	-0.85 – 3.18	0.257			
Symptoms (Yes)							0.32	-0.27 – 0.91	0.291
Random Effects									
σ^2	0.54			0.54			0.55		
τ_{00}	0.97 $_{\text{Subject:Study}}$			0.96 $_{\text{Subject:Study}}$			0.94 $_{\text{Subject:Study}}$		
	0.73 $_{\text{Study}}$			0.73 $_{\text{Study}}$			0.50 $_{\text{Study}}$		
ICC	0.76			0.76			0.72		
N	109 $_{\text{Subject}}$			109 $_{\text{Subject}}$			109 $_{\text{Subject}}$		
	4 $_{\text{Study}}$			4 $_{\text{Study}}$			4 $_{\text{Study}}$		
Observations	812			812			812		
Marginal R^2 / Conditional R^2	0.030 / 0.766			0.037 / 0.766			0.012 / 0.727		

6.3) Effect of Induced Blood Flow Alteration

6.3.1) Tendon and SSCT Motion

Altered blood flow was found to significantly predict FDS displacement ($\beta = -0.118$, $p < 0.01$) (Figure 6.6a) and SSCT displacement ($\beta = -0.116$, $p < 0.01$) (Figure 6.6c). When the type of blood flow alteration was considered, subdiastolic alteration was found to decrease FDS displacement ($\beta = -0.144$, $p < 0.05$) (Figure 6.6b), while supradiastolic alteration was found to decrease SSCT displacement ($\beta = -0.122$, $p < 0.05$) (Figure 6.6d), compared to no altered blood flow. All model results for tendon and SSCT displacements are reported in Table 6.5.

Regarding strain measures, altered blood flow was found to affect shear strain index (SSI). When subjected to subdiastolic blood flow occlusion, SSI increased relative to baseline conditions ($\beta = 3.44$, $p < 0.05$). No significant change was detected with the administration of supradiastolic blood flow alteration. Model results for strain measures are reported in Table 6.6.

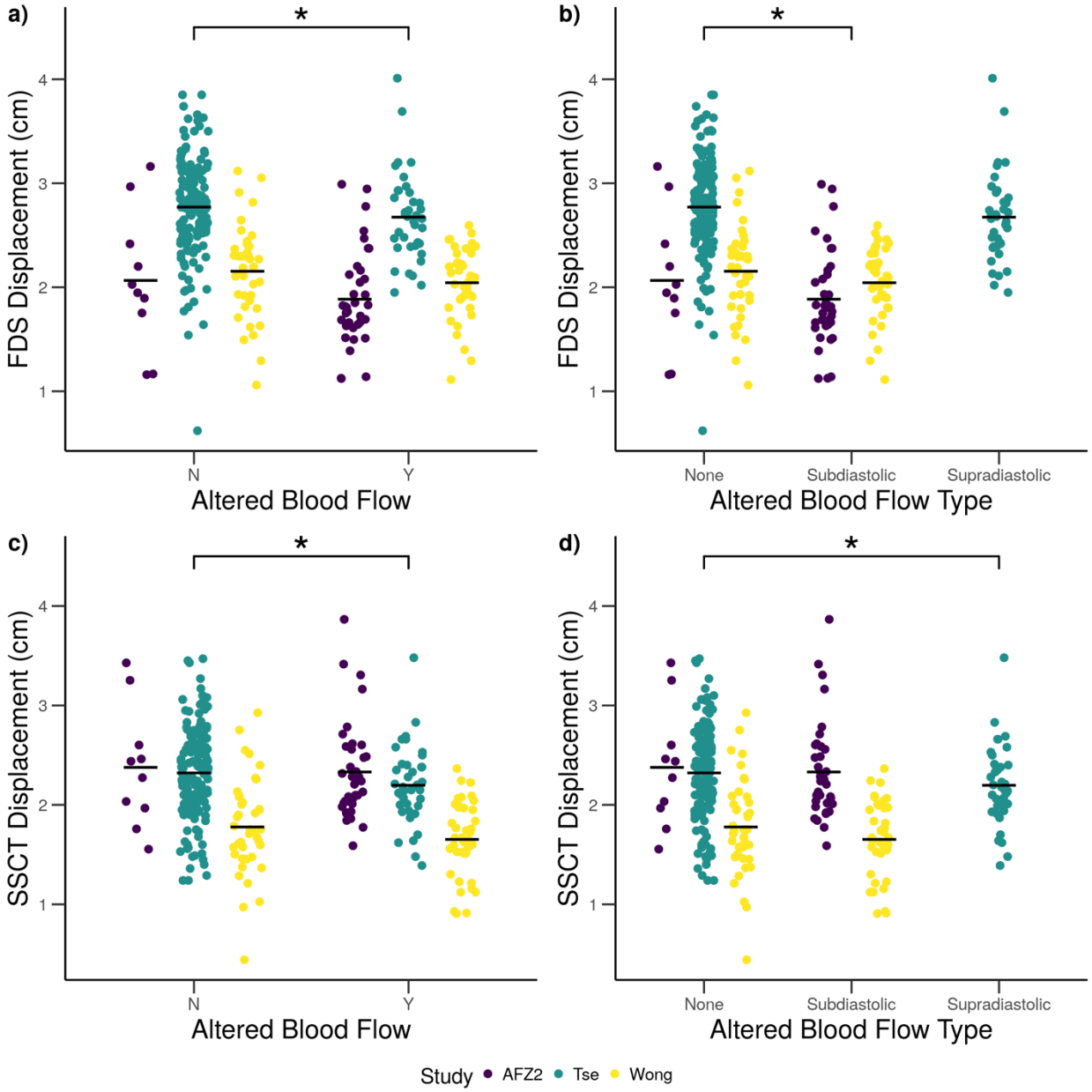

Figure 6.6. Tissue displacements by altered blood flow (left column) and altered blood flow type (right column). Mean values are represented by the horizontal black lines. a) Altered blood flow decreases FDS displacement (N = No blood flow alteration, Y = Yes blood flow alteration). b) Subdiastolic blood flow alteration decreases FDS displacement. c) Altered blood flow decreases SSCT displacement. d) Supradiastolic blood flow alteration decreases SSCT displacement.

Table 6.5. Model results for changes in tissue motion from altered blood flow. Estimates represent the beta-coefficient for the associated predictor variable and are provided with 95% confidence intervals (CI). Significant results are bolded and defined at a level of $p < 0.05$. The intercept represents the estimate for the reference group, and are the following for the predictor variables: Altered Blood Flow, No; Altered Blood Flow Type, None. The between group variance for the random effects are provided in the rows denoted by τ_{00}. Where applicable, individual study results from each model are detailed in Appendix 4.1 – Appendix 4.4.

	FDS Displacement			**FDS Displacement**			**SSCT Displacement**			**SSCT Displacement**		
Predictors	*Estimates*	*CI*	*p*	*Estimates*	*CI*	*p*	*Estimates*	*CI*	*p*	*Estimates*	*CI*	*p*
(Intercept)	2.32	1.85 – 2.78	**<0.001**	2.33	1.88 – 2.78	**<0.001**	2.17	1.77 – 2.56	**<0.001**	2.17	1.77 – 2.56	**<0.001**
Altered Blood Flow (Yes)	-0.12	-0.20 – -0.04	**0.003**				-0.12	-0.20 – -0.03	**0.009**			
Altered Blood Flow Type (Subdiastolic)				-0.14	-0.26 – -0.03	**0.013**				-0.11	-0.24 – 0.02	0.089
Altered Blood Flow Type (Supradiastolic)				-0.09	-0.20 – 0.02	0.092				-0.12	-0.24 – -0.00	**0.047**
Random Effects												
σ^2	0.09			0.09			0.12			0.12		
τ_{00}	0.11 $_{\text{Subject:Study}}$			0.11 $_{\text{Subject:Study}}$			0.10 $_{\text{Subject:Study}}$			0.09 $_{\text{Subject:Study}}$		
	0.16 $_{\text{Study}}$			0.15 $_{\text{Study}}$			0.11 $_{\text{Study}}$			0.11 $_{\text{Study}}$		
N	49 $_{\text{Subject}}$			49 $_{\text{Subject}}$			49 $_{\text{Subject}}$			49 $_{\text{Subject}}$		
	3 $_{\text{Study}}$			3 $_{\text{Study}}$			3 $_{\text{Study}}$			3 $_{\text{Study}}$		
Observations	317			317			317			317		
Marginal R^2 / Conditional R^2	0.009 / 0.743			0.011 / 0.736			0.010 / 0.647			0.009 / 0.646		

Table 6.6. Model results for changes in strain measures from altered blood flow. Estimates represent the beta-coefficient for the associated predictor variable and are provided with 95% confidence intervals (CI). Significant results are bolded and defined at a level of $p < 0.05$. The intercept represents the estimate for the reference group, and are the following for the predictor variables: Altered Blood Flow, No; Altered Blood Flow Type, None. The between group variance for the random effects are provided in the rows denoted by τ_{00}. Where applicable, individual study results from each model are detailed in Appendix 4.5 – Appendix 4.10.

	Relative Displacement			**Relative Displacement**			**SSI**			**SSI**			**MVR**			**MVR**		
Predictors	*Estimates*	*CI*	*p*	*Estimates*	*CI*	*p*	*Estimates*	*CI*	*p*	*Estimates*	*CI*	*p*	*Estimates*	*CI*	*p*	*Estimates*	*CI*	*p*
(Intercept)	0.50	0.43 – 0.57	**<0.001**	0.50	0.42 – 0.57	**<0.001**	24.47	13.04 – 35.90	**<0.001**	23.95	13.10 – 34.79	**<0.001**	81.29	78.44 – 84.14	**<0.001**	81.55	78.65 – 84.45	**<0.001**
Altered Blood Flow (Yes)	0.02	-0.03 – 0.06	0.504				2.04	-0.10 – 4.18	0.062				-1.62	-3.57 – 0.33	0.103			
Altered Blood Flow Type (Subdiastolic)				0.02	-0.04 – 0.08	0.564				3.44	0.36 – 6.52	**0.029**				-2.59	-5.30 – 0.12	0.061
Altered Blood Flow Type (Supradiastolic)				0.01	-0.05 – 0.08	0.708				0.76	-2.20 – 3.72	0.615				-0.64	-3.36 – 2.08	0.645
	Random Effects																	
σ^2	0.03			0.03			69.57			69.49			59.00			58.98		
τ_{00}	0.04 Subject:Study			0.04 Subject:Study			110.35 Subject:Study			110.43 Subject:Study			83.77 Subject:Study			83.96 Subject:Study		
	0.00 Study			0.00 Study			92.90 Study			82.24 Study			0.00 Study			0.00 Study		
ICC	0.56			0.56			0.75			0.73						0.59		
N	49 Subject			49 Subject			49 Subject			49 Subject			49 Subject			49 Subject		
	3 Study			3 Study			3 Study			3 Study			3 Study			3 Study		
Observations	317			317			317			317			318			318		
Marginal R^2 / Conditional R^2	0.001 / 0.561			0.001 / 0.561			0.004 / 0.746			0.008 / 0.737			0.010 / NA			0.008 / 0.591		

6.3.2) CTS Comparison

All levels of altered blood flow were significantly different from baseline measures (Healthy-T1 vs Healthy, β = -0.91, p <0.001; Healthy-T2 vs Healthy, β = -0.68, p <0.001; Healthy-T3 vs Healthy, β = -0.85, p <0.001; Healthy-T4 vs Healthy, β = -0.91, p <0.001), the Possible group (Healthy-T1 vs Possible, β = -1.12, p < 0.01; Healthy-T2 vs Possible, β = -0.90, p < 0.05; Healthy-T3 vs Possible, β = -1.07, p < 0.01; Healthy-T4 vs Possible, β = -1.13, p < 0.01, and the Follow-Up group (Healthy-T1 vs Follow-Up, β = -2.38, p < 0.05; Healthy-T2 vs Follow-Up, β = -2.15, p < 0.05; Healthy-T3 vs Follow-Up, β = -2.32, p < 0.05; Healthy-T4 vs Follow-Up, β = -2.38, p < 0.05) (Figure 6.7). Refer to Appendix 4.11 and 4.12 for complete model results.

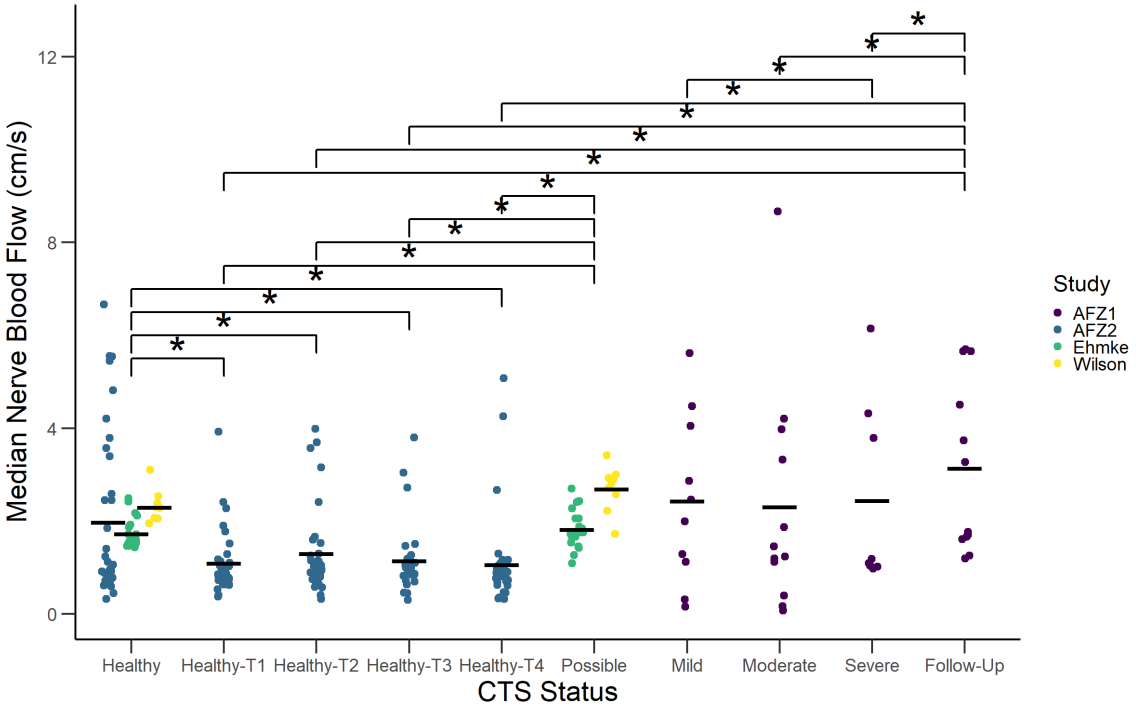

Figure 6.7. Median nerve blood flow velocity for different CTS Status groups. All levels of altered blood flow (Healthy-T1 to Healthy-T4) were significantly different compared to Healthy, Possible, and Follow-Up groups.

7. Discussion

This thesis attempted to consolidate findings from numerous studies conducted within the McMaster Occupational Biomechanics Lab. Specifically, studies that investigated tissue motion and median nerve blood flow in relation to the overall theme of carpal tunnel syndrome (CTS) were considered and implemented in these analyses. Overall, tissues that are associated with CTS pathology—that is, the FDS tendon and surrounding SSCT—demonstrate altered motion as a result of changes to biomechanical factors. Median nerve blood flow, another metric of interest, was found to differ amongst different samples, with deviated wrist postures, and differences in fingertip force. Relating these concepts of tissue motion and blood flow is local blood/fluid flow alteration, which was demonstrated to influence tissue motions when used as an intervention.

7.1) Biomechanical Influences on Tendon and SSCT Motion

Previously, movement speed was treated as a categorical factor with the levels being the speeds or frequencies demanded by subjects in their respective study protocols. In these analyses, tissue velocities were used in place of demanded speed/frequency to assess the effect of movement speed. Effectively, this addressed the differences in the wide range of movement speeds, generated a larger dataset, and provided a more definitive and generalizable statement to be made regarding the speed-displacement relationship for the FDS tendon and SSCT.

7.1.1) FDS Displacement

A negative relationship was demonstrated between velocity and displacement of the FDS tendon (Figure 6.1a). Given the same range of motion, the faster the FDS

tendon moves, the lower the displacement of the tendon that occurs. This result may potentially be attributed to the viscoelastic properties of tendons, where higher strain rates are accompanied by a greater stiffness (Wu, 2006). Thus, for the same required range of motion, there is less displacement of the tendon overall with greater movement speed due to a reduction in strain.

Wrist posture was also found to influence FDS displacement, where wrist flexion decreased displacement (Figure 6.1b). This mirrors findings in cadaveric samples where flexion was found to reduce the extent of tendon excursion (Yoshii, Zhao, Zhao, et al., 2008). It is possible that volar movement of the FDS tendon with wrist flexion (Gabra, Gordon, Marquardt, & Li, 2016; Yoshii, Zhao, Zhao, et al., 2008) reduces the moment arm of the tendon at the wrist, effectively reducing tendon excursion for the same range of finger motion (An, 2007).

Measurements of FDS tendon displacements in these samples of data primarily ranged from 1-4 cm (Figure 6.1), with an overall mean of 2.48 cm (Table 6.1). This corresponds to literature values of mean peak FDS displacements, of which include: 2.1 cm (van Beek et al., 2018); 1.84 cm (Filius et al., 2017); 1.88 cm for CTS cases and 1.56 cm for controls (Filius et al., 2015); 1.98 (0.28-3.88) cm for CTS cases and 1.38 (0.0-3.66) cm for controls (Korstanje et al., 2012); ~3.3 cm (Yoshii et al., 2011); ~1-4 cm (Yoshii, Villarraga, et al., 2009); ~3-4 cm pre- and post-surgery (Yoshii, Zhao, et al., 2009); 2.61 cm for CTS hands, 2.52 cm for cadaver CTS hands, and 2.44 cm for cadaver control hands (Ettema et al., 2008); and ~1.5-2 cm (Ugbolue et al., 2005).

7.1.2) SSCT Displacement

Changes to SSCT displacement closely followed those of the FDS tendon, with a reduction in displacement with greater SSCT velocity (once outliers were removed) (Figure 6.2a), as well as with a flexed wrist posture (Figure 6.2b). It is likely this change is evidence of accommodation by the SSCT to the demand of greater tendon excursion velocity, as the SSCT primarily functions to support smooth tendon gliding within the carpal tunnel.

The SSCT displacements measured in these studies were once again in the range of 1-4 cm (Figure 6.2). Unlike FDS displacement, raw values for SSCT displacement are not as widely published, with some examples being: 1.3 cm for controls and 1.55 cm for CTS patients (Korstanje et al., 2012); ~0.5 cm in cadaveric specimens (Yoshii, Zhao, et al., 2009); 0.69 cm for CTS hands, 0.78 cm for cadaver CTS hands, and 0.90 cm for cadaver control hands (Ettema et al., 2008); and 0.64-1.20 cm pre-surgery, and 0.85-1.18 cm post-surgery (Yoshii et al., 2008). Some of the difference in values between the present studies and those from the literature may be attributed to the demanded speed of motion. Where this thesis assessed SSCT motions of up to 16 cm/s, others have tested and documented motions of 0.2-1.0 cm/s (Yoshii et al., 2011), and 0.2 cm/s (Yoshii et al., 2008), falling on the extreme low end of the spectrum in the current study.

7.1.3) Strain Measures

The use of the term "strain measures" in this document refer to outcomes that attempt to quantify damage to the SSCT via the shear-strain mechanism of injury, and represent some form of relative motion where a disconnect in the motion of the FDS

tendon and SSCT promotes SSCT damage. Collectively, these outcomes include relative displacement, the shear strain index (SSI), and the maximum velocity ratio (MVR). FDS velocity was found to significantly predict relative displacement, SSI, and MVR (Table 6.2), with greater velocity being associated with greater relative displacement, greater SSI, and lesser MVR. Meanwhile, greater SSCT velocity was only found to predict a lower MVR (Figure 6.3). Despite FDS velocity predicting an elevated risk for shear-strain injury across a greater number of metrics compared to SSCT velocity, it is important to take note of each predictor's weighting in these measures. In the cases of relative displacement and MVR, each predictor is given an equal weighting, where relative displacement is simply the arithmetic difference between FDS and SSCT displacements, and MVR the quotient of SSCT and FDS velocity. Meanwhile, SSI takes the quotient of relative displacement and FDS displacement, allocating greater weight to FDS motion compared to the SSCT. Thus, it is necessary to stress caution on the use of SSCT motion as a predictor of SSI due to the greater weighting of FDS displacement, and to perhaps go so far as to avoid the use of this metric as a surrogate for the risk of SSCT damage.

7.2) Median Nerve Blood Flow Changes

7.2.1) Biomechanical Influences on Median Nerve Blood Flow

With wrist flexion, median nerve blood flow velocity was found to increase compared to a neutral wrist posture (Figure 6.4a). Acting as a surrogate for carpal tunnel pressure, a change to median nerve blood flow velocity can be interpreted as having functional outcomes to the median nerve relating to CTS. Greater fingertip force has been linked to an elevation in carpal tunnel pressure, with a doubling of pressure from

about 20 mmHg at 0 N force, to about 40 mmHg at 6 N of fingertip force in a pronated forearm posture (Rempel, Keir, Smutz, & Hargens, 1997). Coincidentally, the data analysed for this thesis measured median nerve blood flow with 6 N of fingertip force, which was demonstrated to increase median nerve blood flow velocity compared to 0 N of fingertip force (Figure 6.4b). However, despite fingertip force elevating both carpal tunnel pressure and median nerve blood flow independently, it may be inappropriate to assume these outcomes happen in tandem.

Overall, a fair interpretation of the results may be that median nerve blood flow increases with fingertip force to support the greater active demands of the muscles it innervates (in this specific case, the FDS muscle). Meanwhile, in passive circumstances, median nerve blood flow decreases with greater carpal tunnel pressure, and subsequently increases the severity of symptoms in individuals with CTS. The manner in which intraneural blood flow of the median nerve decreases may arise in a multitude of ways: from a net decrease to the nerve due to greater arteriovenous flow through fistulous connections (Joy et al., 2011), to neovascularization and a greater number of blood vessels (Gupta et al., 2005; Mohammadi, Ghasemi-Rad, Mladkova-Suchy, & Ansari, 2012; Vanderschueren, Meys, & Beekman, 2014).

7.2.2) Group Differences

Given subjects characterized as healthy, possible (i.e., undiagnosed but experience symptoms), confirmed cases of CTS, and a 6-month follow-up group of CTS patients, the only difference amongst groups was between CTS and Follow-Up individuals (Figure 6.5a). Unlike initially hypothesized, CTS subjects did not demonstrate higher median

nerve blood flow velocity compared to healthy and symptomatic (possible) individuals. Further dissemination of confirmed CTS cases into their respective severities (Figure 6.5b) continued to show no difference in median nerve blood flow for CTS cases compared to the healthy and possible groups. Despite this, differences are present between the mild and severe, moderate and follow-up, and severe and follow-up groups. Finally, the presence of symptoms was not effective as a predictor for median nerve blood flow (Table 6.4). This investigation underlies the importance of classification of CTS groups: how experiencing symptoms alone may not be sufficient to predict median nerve blood flow, and that subtle differences associated with the severity of a CTS diagnosis can change median nerve blood flow.

Overall, there appears to be a decline in median nerve blood flow as CTS severity increases, which matches the findings by Evans and colleagues (2012). Additionally, median nerve blood flow levels in the follow-up group rose to approximately the same as those of the mild group (Figure 6.5b). Physiologically, this may be an indication that insufficient blood flow to the median nerve is responsible for increasing the severity of symptoms experienced by individuals with CTS, which can be partially alleviated with interventions such as splitting of the wrist. This is further supported by findings such as greater contact pressure on the median nerve increasing symptom severity (Lundborg et al., 1982), and a dose-response relationship of pressure on median nerve dysfunction having been established in a rabbit model (Diao et al., 2005).

7.3) Effect of Induced Blood Flow Alteration

To understand how the local fluid environment in the carpal tunnel affects tissue motion and potential injury of carpal tunnel structures, altered blood flow was induced using subdiastolic occlusion or supradiastolic partial ischemia. Notably, any type of experimentally altered blood flow was found to change FDS tendon and SSCT displacements (Figure 6.6), demonstrating the effectiveness of the intervention to elicit a response. Differences in the effects of the blood flow alteration were observed in tissue motion. For the FDS tendon, only subdiastolic occlusion was found to reduce displacement (Figure 6.6b). Meanwhile, for the SSCT, only supradiastolic pressure was found to reduce displacement (Figure 6.6d). These findings may suggest a crucial threshold exists in the hydrostatic pressure within the carpal tunnel that differentially affects tendon and SSCT motion. However, it is important to stress the spread of the data are incredibly close between both subdiastolic and supradiastolic blood flow alteration, with confidence intervals of -0.26 – -0.03 (subdiastolic) and -0.20 – 0.02 (supradiastolic) for FDS displacement, and -0.24 – 0.02 (subdiastolic) and -0.24 – 0.02 (supradiastolic) for SSCT displacement (Table 6.7). Thus, it may be possible these differences primarily emerged from variability between subjects.

Consequences to changes in carpal tunnel tissue motion were observed with subdiastolic occlusion, where SSI was found to increase relative to baseline conditions (Table 6.8). This suggests altered blood flow affects the local fluid environment in the carpal tunnel to promote shear injury to the SSCT. Physiologically, this may be explained by the hydrophilic properties of the SSCT due to its histological composition

(Guimberteau et al., 2010), that promote tissue swelling of the SSCT and lead to less displacement.

When comparing median nerve blood flow from healthy subjects undergoing local blood flow alteration to subjects with varying degrees of CTS severity, differences emerged between the altered blood flow subjects and Healthy (baseline), Possible, and Follow-Up groups (Figure 6.7). Meanwhile, the altered blood flow subjects were not significantly different from confirmed CTS subjects with Mild, Moderate, and Severe classifications. This may imply the subdiastolic occlusion condition utilized by Farias Zuniga (2020) more closely mimics individuals with confirmed CTS at a stage that requires surgery.

7.4) Limitations

Ultimately, while cohorts from multiple studies were combined to increase the sample for analysis, and predictor variables were limited for each model to allow for greater inclusion of studies, some changes were largely driven by data from a few cohorts. Additionally, the majority of subjects were collected from a healthy university population, with a smaller subset of the total dataset from those with CTS symptoms, confirmed subjects with CTS, and cadaveric specimens. This may limit the generalizability of the results to the broader population.

8. Conclusion

This thesis assessed the effects of biomechanical influences on carpal tunnel tissue motion and median nerve blood flow, and attempted to bridge our understanding of their effects upon one another by analysing the effect of induced blood flow alteration in the carpal tunnel. Reductions in FDS tendon and SSCT displacement were identified with increasing tissue velocity and flexed wrist postures. Accompanying these changes to tissue motion were greater strain, represented by higher relative displacement and SSI with increasing FDS velocity, as well as lower MVR with increasing tissue velocity. When median nerve blood flow changes were assessed, force generation and flexed wrist postures were found to reduce blood flow. The classification of CTS groups was found to be a contributor to differences in median nerve blood flow when CTS status was used as a predictor. Finally, induced blood flow alteration was characterized by median nerve blood flow reminiscent of a subject with CTS, and a greater risk of damage occurring to the SSCT.

9. References

An, K.-N. (2007). Tendon excursion and gliding: Clinical impacts from humble concepts. *Journal of Biomechanics*, *40*(4), 713–718. https://doi.org/10.1016/j.jbiomech.2006.10.008

Atroshi, I., Gummesson, C., Johnsson, R., Ornstein, E., Ranstam, J., & Rosén, I. (1999). Prevalence of carpal tunnel syndrome in a general population. *Journal of the American Medical Association*, *282*(2), 153–158. https://doi.org/10.1001/jama.282.2.153

Bower, J. A., Stanisz, G. J., & Keir, P. J. (2006). An MRI evaluation of carpal tunnel dimensions in healthy wrists: Implications for carpal tunnel syndrome. *Clinical Biomechanics*, *21*(8), 816–825. https://doi.org/10.1016/j.clinbiomech.2006.04.008

Cobb, T. K., An, K., & Cooney, W. P. (1995). Effect of Lumbrical Muscle Incursion Within the Carpal Tunnel on Carpal Tunnel Pressure : A Cadaveric Study. *The Journal of Hand Surgery*, *20*(2), 186–192. Retrieved from http://www.sciencedirect.com/science/article/pii/S036350230580005X

Dale, A. M., Harris-Adamson, C., Rempel, D., Gerr, F., Hegmann, K., Silverstein, B., … Evanoff, B. (2013). Prevalence and incidence of carpal tunnel syndrome in US working populations: pooled analysis of six prospective studies. *Scandinavian Journal of Work, Environment & Health*, *39*(5), 495–505. https://doi.org/10.5271/sjweh.3351

Diao, E., Shao, F., Liebenberg, E., Rempel, D., & Lotz, J. C. (2005). Carpal tunnel pressure alters median nerve function in a dose-dependent manner: A rabbit model for carpal tunnel syndrome. *Journal of Orthopaedic Research*, *23*(1), 218–223. https://doi.org/10.1016/j.orthres.2004.05.014

Ehmke, S., Farias Zuniga, A., & Keir, P. J. (2020). Effect of Force, Posture, and Repetitive Wrist Motion on Intraneural Blood Flow in the Median Nerve. *Journal of Ultrasound in Medicine*, 1–12. https://doi.org/10.1002/jum.15467

Ettema, A. M., Amadio, P. C., Zhao, C., Wold, L. E., & An, K.-N. (2004). A histological and immunohistochemical study of the subsynovial connective tissue in idiopathic carpal tunnel syndrome. *The Journal of Bone and Joint Surgery. American Volume*, *86*(7), 1458–1466. https://doi.org/10.1016/j.clinbiomech.2007.07.009

Ettema, A. M., Amadio, P. C., Zhao, C., Wold, L. E., O'Byrne, M. M., Moran, S. L., & An, K.-N. (2006). Changes in the Functional Structure of the Tenosynovium in Idiopathic Carpal Tunnel Syndrome: A Scanning Electron Microscope Study. *Plastic and Reconstructive Surgery*, *118*(6), 1413–1422. https://doi.org/10.1097/01.prs.0000239593.55293.c7

Ettema, A. M., An, K.-N., Zhao, C., O'Byrne, M. M., & Amadio, P. C. (2008). Flexor Tendon and Synovial Gliding During Simultaneous and Single Digit Flexion in Idiopathic Carpal Tunnel Syndrome. *Journal of Biomechanics*, *41*(2), 292–298. Retrieved from https://www.ncbi.nlm.nih.gov/pmc/articles/PMC2254138/pdf/nihms-39438.pdf

Evans, K. D., Roll, S. C., Volz, K. R., & Freimer, M. (2012). Relationship Between Intraneural Vascular Flow Measured With Sonography and Carpal Tunnel Syndrome Diagnosis Based on Electrodiagnostic Testing. *Journal of Ultrasound in Medicine*, *31*(5), 729–736.

Evans, K. D., Volz, K. R., Hutmire, C., & Roll, S. C. (2012). Morphologic characterization of intraneural flow associated with median nerve pathology. *Journal of Diagnostic Medical Sonography*, *28*(1), 11–19. https://doi.org/10.1177/8756479311426777

Farias Zuniga, A. (2020). *Carpal tunnel pathomechanics: vascular dynamics, tissue kinematics, & nerve function*.

Farias Zuniga, A., Ghavanini, A. A., Israelian, G., & Keir, P. J. (2020). Blood flow velocity but not tendon mechanics relates to nerve function in carpal tunnel syndrome patients. *Journal of the Neurological Sciences*, *411*, 1–10. https://doi.org/10.1016/j.jns.2020.116694

Filius, A., Thoreson, A. R., Ozasa, Y., An, K. N., Zhao, C., & Amadio, P. C. (2017). Delineation of the mechanisms of tendon gliding resistance within the carpal tunnel. *Clinical Biomechanics*, *41*, 48–53. https://doi.org/10.1016/j.clinbiomech.2016.12.001

Filius, A., Thoreson, A. R., Wang, Y., Passe, S. M., Zhao, C., An, K.-N., & Amadio, P. C. (2015). The Effect of Tendon Excursion Velocity on Longitudinal Median Nerve Displacement: Differences Between Carpal Tunnel Syndrome Patients and Controls. *Journal of Orthopedic Research*, *33*(4), 483–487. https://doi.org/10.1002/jor.22804

Freeland, A. E., Tucci, M. A., Barbieri, R. A., Angel, M. F., & Nick, T. G. (2002). Biochemical evaluation of serum and flexor tenosynovium in carpal tunnel syndrome. *Microsurgery*, *22*(8), 378–385. https://doi.org/10.1002/micr.10065

Gabra, J. N., Gordon, J. L., Marquardt, T. L., & Li, Z. M. (2016). In vivo tissue interaction between the transverse carpal ligament and finger flexor tendons. *Medical Engineering and Physics*, *38*(10), 1055–1062. https://doi.org/10.1016/j.medengphy.2016.06.023

Garg, A., Moore, J. S., & Kapellusch, J. M. (2017). The Revised Strain Index: an improved upper extremity exposure assessment model. *Ergonomics*, *60*(7), 912–922. https://doi.org/10.1080/00140139.2016.1237678

Gelberman, R. H., Hergenroeder, P. T., Hargens, A. R., Lundborg, G. N., & Akeson, W. H. (1981). The carpal tunnel syndrome: A study of carpal canal pressures. *The Journal of Bone and Joint Surgery*, *63-A*(3), 380–383. https://doi.org/10.1016/0049-0172(71)90012-6

Guimberteau, J. C., Delage, J. P., McGrouther, D. A., & Wong, J. K. F. (2010). The microvacuolar system: how connective tissue sliding works. *The Journal of Hand Surgery (European Volume)*, *35*(8), 614–622. Retrieved from https://journals-scholarsportal-info.libaccess.lib.mcmaster.ca/pdf/17531934/v35i0008/614_tmshctsw.xml

Gupta, R., Gray, M., Chao, T., Bear, D., Modafferi, E., & Mozaffar, T. (2005). Schwann cells upregulate vascular endothelial growth factor secondary to chronic nerve compression injury. *Muscle and Nerve*, *31*(4), 452–460. https://doi.org/10.1002/mus.20272

Jinrok, O., Zhao, C., Amadio, P. C., An, K.-N., Zobitz, M. E., & Wold, L. E. (2004). Vascular pathologic changes in the flexor tenosynovium (subsynovial connective tissue) in idiopathic carpal tunnel syndrome. *Journal of Orthopaedic Research*, *22*(6), 1310–1315. https://doi.org/10.1016/j.orthres.2004.03.005

Joy, V., Therimadasamy, A. K., Chan, Y. C., & Wilder-Smith, E. P. (2011). Combined Doppler and B-mode sonography in carpal tunnel syndrome. *Journal of the Neurological Sciences*, *308*(1–2), 16–20. https://doi.org/10.1016/j.jns.2011.06.042

Keir, P. J., & Bach, J. M. (2000). Flexor muscle incursion into the carpal tunnel: A mechanism for increased carpal tunnel pressure? *Clinical Biomechanics*, *15*(5), 301–305. https://doi.org/10.1016/S0268-0033(99)00092-3

Keir, P. J., Bach, J. M., & Rempel, D. M. (1998). Effects of finger posture on carpal tunnel pressure during wrist motion. *The Journal of Hand Surgery*, *23*(6), 1004–1009. https://doi.org/10.1016/S0363-5023(98)80007-5

Keir, P. J., Farias Zuniga, A., Mulla, D. M., & Somasundram, K. G. (2019). Relationships and Mechanisms Between Occupational Risk Factors and Distal Upper Extremity Disorders. *Human Factors*, 1–27. https://doi.org/10.1177/0018720819860683

Kociolek, A. M., & Keir, P. J. (2016). Relative motion between the flexor digitorum superficialis tendon and paratenon in zone V increases with wrist flexion angle. *Journal of Orthopaedic Research*, *34*(7), 1248–1255. https://doi.org/10.1002/jor.23133

Kociolek, A. M., Tat, J., & Keir, P. J. (2015). Biomechanical risk factors and flexor tendon frictional work in the cadaveric carpal tunnel. *Journal of Biomechanics*, *48*(3), 449–455. https://doi.org/10.1016/j.jbiomech.2014.12.029

Korstanje, J.-W. H., Scheltens-De Boer, M., Blok, J. H., Amadio, P. C., Hovius, S. E., Stam, H. J., & Selles, R. W. (2012). Ultrasonographic Assessment of Longitudinal Median Nerve and Hand Flexor Tendon Dynamics in Carpal Tunnel Syndrome. *Muscle Nerve*, *45*(5), 721–729. https://doi.org/10.1002/mus.23246

Kuznetsova, A., Brockhoff, P. B., & Christensen, R. H. B. (2017). lmerTest Package: Tests in Linear Mixed Effects Models. *Journal of Statistical Software*, *82*(13), 1–26. https://doi.org/10.18637/jss.v082.i13

Luchetti, R., Schoenhuber, R., Cicco, G. De, Alfarano, M., Deluca, S., & Landi, A. (1989). Carpal-tunnel pressure. *Acta Orthopaedica*, *60*(4), 397–399. https://doi.org/10.3109/17453678909149305

Lundborg, G. (1975). Structure and Function of the Intraneural Microvessels as Related to Trauma, Edema Formation, and Nerve Function. *The Journal of Bone and Joint Surgery*, *57-A*(7), 938–948.

Lundborg, G., Gelberman, R. H., Minteer-Convery, M., Lee, Y. F., & Hargens, A. R. (1982). Median nerve compression in the carpal tunnel—Functional response to experimentally induced controlled pressure. *Journal of Hand Surgery*, *7*(3), 252–259. https://doi.org/10.1016/S0363-5023(82)80175-5

Mogk, J. P. M., & Keir, P. J. (2008). Wrist and carpal tunnel size and shape measurements: Effects of posture. *Clinical Biomechanics*, *23*(9), 1112–1120. https://doi.org/10.1016/j.clinbiomech.2008.05.009

Mohammadi, A., Ghasemi-Rad, M., Mladkova-Suchy, N., & Ansari, S. (2012). Correlation between the severity of carpal tunnel syndrome and color doppler sonography findings. *American Journal of Roentgenology*, *198*(2), 181–184. https://doi.org/10.2214/AJR.11.7012

Motomiya, M., Funakoshi, T., Ishizaka, K., Nishida, M., Matsui, Y., & Iwasaki, N. (2018). Blood flow changes in subsynovial connective tissue on contrast-enhanced ultrasonography in patients with carpal tunnel syndrome before and after surgical decompression. *Journal of Ultrasound in Medicine*, *37*(7), 1597–1604. https://doi.org/10.1002/jum.14500

Musolin, K. M., & Ramsey, J. G. (2017). Carpal tunnel syndrome prevalence: an evaluation of workers at a raw poultry processing plant. *International Journal of Occupational and Environmental Health*, *23*(4), 282–290. https://doi.org/10.1080/10773525.2018.1474420

Nakagawa, S., & Schielzeth, H. (2013). *A general and simple method for obtaining R 2 from generalized linear mixed-effects models*. *2*, 133–142. https://doi.org/10.1111/j.2041-210x.2012.00261.x

Neal, N. C., McManners, J., & Stirling, G. A. (1987). Pathology of the Flexor Tendon Sheath in the Spontaneous Carpal Tunnel Syndrome. *The Journal of Hand Surgery*, *12*(2), 229–232. Retrieved from https://journals-scholarsportal-info.libaccess.lib.mcmaster.ca/pdf/02667681/v12i0002/229_potftsitscts.xml

Oh, S., Belohlavek, M., Zhao, C., Osamura, N., Zobitz, M. E., An, K. N., & Amadio, P. C. (2007). Detection of differential gliding characteristics of the flexor digitorum superficialis tendon and subsynovial connective tissue using color doppler sonographic imaging. *Journal of Ultrasound in Medicine*, *26*(2), 149–155. https://doi.org/10.7863/jum.2007.26.2.149

Park, G.-Y., Kwon, D. R., Seok, J. I., Park, D.-S., & Cho, H. K. (2018). Usefulness of ultrasound assessment of median nerve mobility in carpal tunnel syndrome. *Acta Radiologica*, *59*(12), 1494–1499. https://doi.org/10.1177/0284185118762246

R Core Team (2021). R: A language and environment for statistical computing. R Foundation for Statistical Computing, Vienna, Austria. URL https://www.R-project.org/.

Rempel, D., Keir, P. J., Smutz, W. P., & Hargens, A. (1997). Effects of Static Fingertip

Loading on Carpal Tunnel Pressure. *The Journal of Bone and Joint Surgery*, *15*, 422–426.

Rempel, D. M., Keir, P. J., & Bach, J. M. (2008). Effect of wrist posture on carpal tunnel pressure while typing. *Journal of Orthopaedic Research*, *26*(9), 1269–1273. https://doi.org/10.1002/jor.20599

Rojviroj, S., Sirichativapee, W., Kowsuwon, W., Wongwiwattananon, J., Tamnanthong, N., & Jeeravipoolvarn, P. (1990). Pressures in the carpal tunnel: A comparison between patients with carpal tunnel syndrome and normal subjects. *The Journal of Bone and Joint Surgery*, *72*(3), 516–518. https://doi.org/10.1302/0301-620x.72b3.2187880

Schuenke, M., Schulte, E., & Schumacher, U. (2010). *Thieme Atlas of Anatomy: General Anatomy and Musculoskeletal System* (L. M. Ross & E. D. Lamperti, eds.). New York: Thieme.

Seiler, J. G., Milek, M. A., Carpenter, G. K., & Swiontkowski, M. F. (1989). Intraoperative assessment of median nerve blood flow during carpal tunnel release with laser Doppler flowmetry. *Journal of Hand Surgery*, *14*(6), 986–991. https://doi.org/10.1016/S0363-5023(89)80048-6

Shiri, R., & Falah-Hassani, K. (2014). Computer use and carpal tunnel syndrome: A meta-analysis. *Journal of the Neurological Sciences*, *349*, 15–19. https://doi.org/10.1016/j.jns.2014.12.037

Silverstein, B. A., Fine, L. J., & Armstrong, T. J. (1987). Occupational factors and carpal tunnel syndrome. *American Journal of Industrial Medicine*, *11*(3), 343–358. https://doi.org/10.1002/ajim.4700110310

Soejima, O., Iida, H., & Naito, M. (2001). Measurement of Median Nerve Blood Flow during Carpal Tunnel Release with Laser Doppler Flowmetry. *Minimally Invasive Neurosurgey*, *44*(4), 202–204.

Tacani, P. M., de Oliveira Ribeiro, D., Guimarães, B. E. B., Machado, A. F. P., & Tacani, R. E. (2015). Characterization of symptoms and edema distribution in premenstrual syndrome. *International Journal of Women's Health*, *7*, 297–303. https://doi.org/10.2147/IJWH.S74251

Tat, J., Kociolek, A. M., & Keir, P. J. (2013). Repetitive differential finger motion increases shear strain between the flexor tendon and subsynovial connective tissue. *Journal of Orthopaedic Research*, *31*(10), 1533–1539. https://doi.org/10.1002/jor.22391

Tat, J., Kociolek, A. M., & Keir, P. J. (2015). Validation of Color Doppler Sonography for Evaluating Relative Displacement Between the Flexor Tendon and Subsynovial Connective Tissue. *Journal of Ultrasound in Medicine*, *34*(4), 679–687. https://doi.org/10.7863/ultra.34.4.679

Tat, J., Kociolek, A. M., & Keir, P. J. (2016). Relative displacement of the tendon and subsynovial connective tissue using ultrasound captures different phenomena than mechanical tendon shear. *Journal of Biomechanics*, *49*(15), 3682–3687.

https://doi.org/10.1016/j.jbiomech.2016.09.038

Tat, J., Wilson, K. E., & Keir, P. J. (2015). Pathological changes in the subsynovial connective tissue increase with self-reported carpal tunnel syndrome symptoms. *Clinical Biomechanics*, *30*(4), 360–365. https://doi.org/10.1016/j.clinbiomech.2015.02.015

Tse, C. T. F., & Keir, P. J. (2020). External Compression and Partial Ischemia Decrease Human Finger Flexor Tendon and Subsynovial Connective Tissue Relative Motion. *Journal of Orthopaedic Research : Official Publication of the Orthopaedic Research Society*, *38*(5), 1038–1044. https://doi.org/10.1002/jor.24540

Ugbolue, U. C., Hsu, W.-H., Goitz, R. J., & Li, Z.-M. (2005). Tendon and nerve displacement at the wrist during finger movements. *Clinical Biomechanics*, *20*, 50–56. https://doi.org/10.1016/j.clinbiomech.2004.08.006

van Beek, N., Gijsbertse, K., Selles, R. W., de Korte, C. L., Veeger, D. J. (H E. J.)., Stegeman, D. F., & Maas, H. (2018). Tendon displacements during voluntary and involuntary finger movements. *Journal of Biomechanics*, *67*, 62–68. https://doi.org/10.1016/j.jbiomech.2017.11.023

van Doesburg, M. H. M., Henderson, J., Yoshii, Y., van der Molen, A. B. M., Cha, S. S., An, K. N., & Amadio, P. C. (2012). Median nerve deformation in differential finger motions: Ultrasonographic comparison of carpal tunnel syndrome patients and healthy controls. *Journal of Orthopaedic Research*, *30*(4), 643–648. https://doi.org/10.1002/jor.21562

Vanderschueren, G. A. K. B., Meys, V. E. W. H., & Beekman, R. (2014). Doppler sonography for the diagnosis of carpal tunnel syndrome: A critical review. *Muscle and Nerve*, *50*(2), 159–163. https://doi.org/10.1002/mus.24241

Wilson, D., & Allen, G. M. (2012). Imaging of the Carpal Tunnel. *Seminars in Musculoskeletal Radiology*, *16*(2), 137–145. https://doi.org/10.1055/s-0032-1311765

Wilson, K. E., Tat, J., & Keir, P. J. (2017). Effects of Wrist Posture and Fingertip Force on Median Nerve Blood Flow Velocity. *BioMed Research International*, *2017*, 1–8. https://doi.org/10.1155/2017/7156489

Wong, A. Y. W., Farias Zuniga, A., & Keir, P. J. (2019). Subdiastolic venous occlusion alters FDS tendon and SSCT mechanics. *International Society of Biomechanics/American Society of Biomechanics (ISB/ASB 2019)*.

Wu, J. J. (2006). Quantitative constitutive behaviour and viscoelastic properties of fresh flexor tendons. *International Journal of Artificial Organs*, *29*(9), 852–857. https://doi.org/10.1177/039139880602900906

Yayama, T., Kobayashi, S., Nakanishi, Y., Uchida, K., Kokubo, Y., Miyazaki, T., … Baba, H. (2010). Effects of graded mechanical compression of rabbit sciatic nerve on nerve blood flow and electrophysiological properties. *Journal of Clinical Neuroscience*, *17*(4), 501–505. https://doi.org/10.1016/j.jocn.2009.07.110

Yoshii, Y., Villarraga, H. R., Henderson, J., Zhao, C., An, K.-N., & Amadio, P. C. (2009). Speckle tracking ultrasound for assessment of the relative motion of flexor tendon and subsynovial connective tissue in the human carpal tunnel. *Ultrasound in Medicine & Biology*, *35*(12), 1973–1981. https://doi.org/10.1016/j.ultrasmedbio.2009.07.004

Yoshii, Y., Zhao, C., Henderson, J., Zhao, K. D., An, K.-N., & Amadio, P. C. (2009). Shear Strain and Motion of the Subsynovial Connective Tissue and Median Nerve During Single Digit Motion. *J Hand Surg Am*, *34*(1), 1–14. https://doi.org/10.1016/j.jhsa.2008.09.021

Yoshii, Y., Zhao, C., Henderson, J., Zhao, K. D., An, K. N., & Amadio, P. C. (2011). Velocity-dependent changes in the relative motion of the subsynovial connective tissue in the human carpal tunnel. *Journal of Orthopaedic Research*, *29*(1), 62–66. https://doi.org/10.1002/jor.21181

Yoshii, Y., Zhao, C., Henderson, J., Zhao, K. D., Zobitz, M. E., An, K.-N., & Amadio, P. C. (2008). Effects of Carpal Tunnel Release on the Relative Motion of Tendon, Nerve, and Subsynovial Connective Tissue in a Human Cadaver Model. *Clinical Biomechanics*, *23*(9), 1121–1127. https://doi.org/10.1016/j.clinbiomech.2008.06.006

Yoshii, Y., Zhao, C., Zhao, K. D., Zobitz, M. E., An, K. N., & Amadio, P. C. (2008). The effect of wrist position on the relative motion of tendon, nerve, and subsynovial connective tissue within the carpal tunnel in a human cadaver model. *Journal of Orthopaedic Research*, *26*(8), 1153–1158. https://doi.org/10.1002/jor.20640

Yung, M., Dale, A. M., Kapellusch, J., Bao, S., Harris-Adamson, C., Meyers, A. R., … Evanoff, B. A. (2019). Modeling the Effect of the 2018 Revised ACGIH® Hand Activity Threshold Limit Value® (TLV) at Reducing Risk for Carpal Tunnel Syndrome. *Journal of Occupational and Environmental Hygiene*, *16*(9), 628–633. https://doi.org/10.1080/15459624.2019.1640366

10. Appendices

Appendix 1

Experimental studies conducted in the McMaster Occupational Biomechanics Lab considered for data inclusion in investigations. Details of population (CTS Status), independent variables tested, dependent variables measured, and a summary of major findings are included.

Authors	Year	Population	Independent Variables	Dependent Variables	Major findings

Farias Zuniga, Ghavanini, Israelian, & Keir	2020	CTS: 35 (27 F, 8 M)	CTS Severity (Mild, Moderate, Severe), Wrist Posture (30° extension, 15° flexion, 0° neutral; finger motion tested only at neutral)	Intraneural BF, Median Nerve CSA, Motor latency, SSCT Motion, Tendon Motion	• Mild CTS severity
					  ○ ↓ motor latency
					  ○ ↑ motor amplitude
					  ○ ↑ conduction velocity
					• Tendon mechanics
					  ○ No relationship with motor latency (indicating motor latency doesn't predict mechanics)
					  ○ Peak FDS, peak SSCT, relative displacement, SSI
					• Blood flow velocity
					  ○ Non-significant (0.054) model for wrist posture predicting blood flow velocity
					  ▪ However, interaction shows peak blood flow velocity greater for non-neutral wrist postures vs neutral only at low motor latencies (3-4.5 ms)
					  • This would be the "mild" severity of CT
					  • No difference b/w flexed and extended wrist postures

Ehkme, Farias Zuniga, & Keir	2020	Healthy: 11 (8 F, 3 M), Symptomatic: 11 (10 F, 1 M)	Grip, Wrist posture, CTS Status	Intraneural BF, Mean arterial pressure	• Grip
					  ○ Forceful grips caused higher blood flow velocities compared to no force
					• Posture
					  ○ Flexed wrist had higher blood flow vs neutral and extended
					• Grip x CTS status interaction (pinch + healthy)

					○ Mean arterial pressure increased with 6 N pinch compared to relaxed and 0 N pinch in healthy but not CTS symptomatic individuals
Wong, Farias Zuniga, & Keir	2019	Healthy: 20 (10F, 10 M)	Blood Flow (Occlusion, Baseline), Movement Speed (0.75 Hz, 1.25 Hz), Biological Sex	Relative Displacement, SSCT Motion, Tendon Motion	• Condition × speed interaction (occlusion + slow speed) ○ Occlusion + slow speed ↓ FDS velocity & displacement, but not SSCT • Main effect of condition (occlusion) ○ Occlusion alone sufficient to ↓ SSCT displacement • Main effect of speed (fast) ○ Fast speed (1.25 Hz) ↓ MVR ○ Fast speed (1.25 Hz) ↓ SSCT displacement
Tse, Keir	2019	Healthy: 19 (9 F, 10 M)	Blood Flow, Mechanical Compression (Forearm, Palmar), Movement Speed (0.75 Hz, 1.25 Hz)	Relative Displacement, SSCT Motion, Tendon Motion	• Main effect of compression (forearm) ○ Forearm compression ↓ FDS displacement • Main effect of blood flow (ischemia) ○ Partial ischemia ↓ SSCT displacement • Main effect of movement speed (fast) ○ Fast speed (1.25 Hz) ↑ relative displacement • SSCT motion ○ Trend for lower displacement with forearm compression
Wilson, Tat, Keir	2017	Healthy: 9 (8 F, 1 M) Symptomatic: 9 (7 F, 2M)	Force (0 N, 6 N), Wrist Posture (30° flexion, 15° flexion, Neutral, 15° extension, 30° extension)	Intraneural BF	• Main effect of wrist posture ○ 30° flexion ↑ median nerve blood flow velocity ○ 15° flexion ↑ median nerve blood flow velocity ○ 30° extension ↑ median nerve blood flow velocity • Main effect of force ○ Middle fingertip force ↑ median nerve blood flow velocity
Kociolek, Keir	2016	Healthy: 16 (8 F, 8 M)	Finger Movement Type (DIP + PIP, MCP, full finger) Wrist Posture (30° Extension, Neutral, 30° Flexion)	Relative Displacement, SSCT Motion, Tendon Motion	• Finger movement type ○ No effect on relative motion • Wrist posture ○ 30° extension ↓ relative displacement ○ 30° flexion ↑ relative displacement
Tat, Kociolek, Keir	2016	Cadaver: 8	Force (10 N, 20 N, 30 N),	Relative Displacement, SSCT Motion,	• Relative displacement increased with tendon frictional work

			Movement Speed (5 cm/s 10 cm/s 15 cm/s), Wrist Posture (Neutral, Flexed)	Tendon Frictional Work, Tendon Motion	• Peak relative displacement and peak frictional work occurred at the end ranges of motion
					• Posture x force interaction on frictional work (force x wrist posture)
					  o Frictional work increased with greater tendon force, but only for flexed (and not neutral) wrist posture
					  o Direct measurement of frictional work
					• Ultrasound measured main effects of posture and force on relative displacement
					  o Flexed wrist had greater relative displacement compared to neutral
					  o 30 N had greater relative displacement compared to 20 N and 10 N
					• Ultrasound measured main effect of movement speed on frictional work and relative displacement
					  o Higher tendon velocities resulted in more frictional work and larger relative displacement

Tat, Kociolek, Keir	2015	Cadaver: 8 (Maybe same as above)	Movement Speed (50 mm/s, 100 mm/s, 150 mm/s)	Relative Displacement, SSCT Motion, Tendon Motion, Measurement error (Colour Doppler tendon displacement – motor displacement)	• Colour Doppler ultrasound accurately measured tendon displacement
					• Measurement error
					  o Flexion phase:
					  ▪ Curvilinear increase in relative displacement towards end range of motion
					  • Possibly due to sequential stretch of fibrils between successive layers of the SSCT
					  o Extension phase:
					  ▪ Linear return in relative displacement
					  • Unloading by uniform relaxation of fibrils

Tat, Wilson, Keir	2015	Healthy: 11 (9F, 2 M), Symptomatic: 11 (9F, 2M)	CTS Status (Symptomatic, Healthy)	SSCT Thickness, Tendon Thickness, Thickness Ratio (SSCT/Tendon), SSI	• CTS Status
					  o Symptomatic ↑ SSCT thickness
					  o Symptomatic ↑ thickness ratio
					  o Symptomatic ↓ SSCT displacement
					  o Symptomatic ↑ SSI
					  o No difference in thickness for FDS or SSCT

Kociolek, Tat, Keir	2015	Cadaver: 8	Force (10 N, 20 N, 40 N),	Tendon Frictional Work	• Wrist posture x tendon force interaction (proximal displacement)

			Movement Speed (50 mm/s, 100 mm/s, 150 mm/s), Wrist Posture (Neutral, 30° Flexion)		○ With increasing tendon force, the increase in tendon frictional work was greater when the wrist was flexed compared to in a neutral posture • Tendon velocity (proximal displacement) ○ Resulted in increase of tendon frictional work during proximal displacement ▪ 58% increase from 50 to 150 mm/s • Wrist posture x tendon velocity x tendon force interaction (distal displacement) ○ Neutral wrist: frictional work increased with tendon velocity, without much effect of tendon force ○ Flexed wrist: frictional work increased with tendon velocity, and increased greater with higher tendon forces • Tendon velocity (distal displacement) ○ Frictional work increased with greater tendon velocity ○ Greater increase with greater tendon force
Tat, Kociolek, Keir	2013	Healthy: 12 (12 M)	Finger Movement Type (Differential, Concurrent), Exertion time (1 min mark, 30 min mark)	MVR, SSCT Motion, SSI, Tendon Motion	• Exertion time ○ Exertion time ↑ FDS displacement in flexion motion ○ Exertion time ↑ SSCT displacement in flexion motion • Movement type ○ Differential motion ↑ **FDS** displacement in flexion motion ○ Concurrent motion ↑ **FDS and SSCT** displacement in flexion motion • Movement type x time interaction for SSI (flexion) ○ Exertion time ↑ SSI for **differential** motion, but not **concurrent** motion • Movement type x time interaction for MVR (flexion & extension) ○ Differential motion ↓ MVR ▪ No change with concurrent motion ▪ Driven by changes in tendon velocity • SSCT velocity stable throughout

Appendix 2.1

Individual study estimates for FDS displacement model with FDS velocity as the predictor. Main model results are denoted in the column "FDS Displacement" and include the effect of Subject nested within Study (Subject:Study) as random effects. Individual study behaviours follow in the columns to the right, and use Subject alone as a random effect. Estimates represent the beta-coefficient for the associated predictor variable and are provided with 95% confidence intervals (CI). Significant results are bolded and defined at a level of $p < 0.05$. The intercept represents the estimate for the reference group, and are the following for the predictor variables: FDS Velocity, 0 cm/s. The between group variance for the random effects are provided in the rows denoted by τ_{00}.

	FDS Displacement			**AFZ2**			**Kociolek (2016)**			**Tat (2016)**			**Tse (2020)**			**Wong (2019)**		
Predictors	*Estimates*	*CI*	*p*	*Estimates*	*CI*	*p*	*Estimates*	*CI*	*p*	*Estimates*	*CI*	*p*	*Estimates*	*CI*	*p*	*Estimates*	*CI*	*p*
(Intercept)	2.48	2.05 – 2.90	**<0.001**	0.45	0.04 – 0.86	**0.030**	0.97	0.52 – 1.43	**<0.001**	3.12	2.98 – 3.25	**<0.001**	3.17	2.89 – 3.44	**<0.001**	1.91	1.55 – 2.27	**<0.001**
FDS Velocity	-0.01	-0.02 – -0.00	**0.004**	0.20	0.14 – 0.25	**<0.001**	0.19	0.12 – 0.26	**<0.001**	-0.02	-0.02 – -0.01	**<0.001**	-0.04	-0.06 – -0.02	**<0.001**	0.02	-0.02 – 0.06	0.272
Random Effects																		
σ^2	0.08			0.06			0.08			0.04			0.08			0.11		
τ_{00}	0.11 $_{\text{Subject:Study}}$ 0.22 $_{\text{Study}}$			0.04 $_{\text{Subject}}$			0.08 $_{\text{Subject}}$			0.02 $_{\text{Subject}}$			0.17 $_{\text{Subject}}$			0.04 $_{\text{Subject}}$		
ICC	0.80			0.40			0.49			0.32			0.68			0.27		
N	73 $_{\text{Subject}}$ 5 $_{\text{Study}}$			10 $_{\text{Subject}}$			16 $_{\text{Subject}}$			8 $_{\text{Subject}}$			19 $_{\text{Subject}}$			20 $_{\text{Subject}}$		
Observations	509			47			48			144			190			80		
Marginal R^2 / Conditional R^2	0.005 / 0.804			0.686 / 0.811			0.333 / 0.659			0.069 / 0.363			0.039 / 0.692			0.015 / 0.281		

Appendix 2.2

Individual study estimates for SSCT displacement model with SSCT velocity as the predictor. Main model results are denoted in the column "SSCT Displacement" and include the effect of Subject nested within the effect of Study (Subject:Study) as random effects. Individual study behaviours follow in the columns to the right, and use Subject alone as a random effect. Estimates represent the beta-coefficient for the associated predictor variable and are provided with 95% confidence intervals (CI). Significant results are bolded and defined at a level of $p < 0.05$. The intercept represents the estimate for the reference group, and are the following for the predictor variables: SSCT Velocity, 0 cm/s. The between group variance for the random effects are provided in the rows denoted by τ_{00}.

	SSCT Displacement			**AFZ2**			**Kociolek (2016)**			**Tat (2016)**			**Tse (2020)**			**Wong (2019)**		
Predictors	*Estimates*	*CI*	*p*	*Estimates*	*CI*	*p*	*Estimates*	*CI*	*p*	*Estimates*	*CI*	*p*	*Estimates*	*CI*	*p*	*Estimates*	*CI*	*p*
(Intercept)	2.04	1.66 – 2.43	**<0.001**	0.47	0.18 – 0.75	**0.001**	1.34	0.98 – 1.69	**<0.001**	3.04	2.89 – 3.19	**<0.001**	3.04	2.74 – 3.33	**<0.001**	1.93	1.55 – 2.31	**<0.001**
SSCT Velocity	-0.01	-0.03 – 0.00	0.096	0.25	0.21 – 0.30	**<0.001**	0.20	0.12 – 0.29	**<0.001**	-0.01	-0.03 – 0.00	0.062	-0.03	-0.06 – -0.01	**0.016**	0.02	-0.03 – 0.08	0.352
Random Effects																		
σ^2	0.13			0.04			0.09			0.05			0.09			0.11		
τ_{00}	0.10 Subject:Study 0.17 Study			0.02 Subject			0.07 Subject			0.02 Subject			0.15 Subject			0.05 Subject		
ICC	0.68			0.31			0.45			0.29			0.64			0.30		
N	73 Subject 5 Study			10 Subject			16 Subject			8 Subject			19 Subject			20 Subject		
Observations	509			47			48			144			190			80		
Marginal R^2 / Conditional R^2	0.004 / 0.680			0.800 / 0.862			0.266 / 0.593			0.020 / 0.303			0.018 / 0.644			0.011 / 0.308		

Appendix 2.3

Individual study estimates for relative displacement with FDS velocity as the predictor. Main model results are denoted in the column "Relative Displacement" and include the effect of Subject nested within the effect of Study (Subject:Study) as random effects. Individual study behaviours follow in the columns to the right, and use Subject alone as a random effect. Estimates represent the beta-coefficient for the associated predictor variable and are provided with 95% confidence intervals (CI). Significant results are bolded and defined at a level of $p < 0.05$. The intercept represents the estimate for the reference group, and are the following for the predictor variables: FDS Velocity, 0 cm/s. The between group variance for the random effects are provided in the rows denoted by τ_{00}.

	Relative Displacement			**AFZ2**			**Tse**			**Wong**		
Predictors	*Estimates*	*CI*	*p*	*Estimates*	*CI*	*p*	*Estimates*	*CI*	*p*	*Estimates*	*CI*	*p*
(Intercept)	0.20	0.05 – 0.35	**0.010**	0.45	0.04 – 0.86	**0.030**	3.17	2.89 – 3.44	**<0.001**	1.91	1.55 – 2.27	**<0.001**
FDS Velocity	0.03	0.03 – 0.04	**<0.001**	0.20	0.14 – 0.25	**<0.001**	-0.04	-0.06 – -0.02	**<0.001**	0.02	-0.02 – 0.06	0.272
Random Effects												
σ^2	0.03			0.06			0.08			0.11		
τ_{00}	0.04 $_{\text{Subject:Study}}$			0.04 $_{\text{Subject}}$			0.17 $_{\text{Subject}}$			0.04 $_{\text{Subject}}$		
	0.01 $_{\text{Study}}$											
ICC	0.63			0.40			0.68			0.27		
N	49 $_{\text{Subject}}$			10 $_{\text{Subject}}$			19 $_{\text{Subject}}$			20 $_{\text{Subject}}$		
	3 $_{\text{Study}}$											
Observations	317			47			190			80		
Marginal R^2 / Conditional R^2	0.115 / 0.673			0.686 / 0.811			0.039 / 0.692			0.015 / 0.281		

Appendix 2.4

Individual study estimates for relative displacement with SSCT velocity as the predictor. Main model results are denoted in the column "Relative Displacement" and include the effect of Subject nested within the effect of Study (Subject:Study) as random effects. Individual study behaviours follow in the columns to the right, and use Subject alone as a random effect. Estimates represent the beta-coefficient for the associated predictor variable and are provided with 95% confidence intervals (CI). Significant results are bolded and defined at a level of $p < 0.05$. The intercept represents the estimate for the reference group, and are the following for the predictor variables: SSCT Velocity, 0 cm/s. The between group variance for the random effects are provided in the rows denoted by τ_{00}.

	Relative Displacement			**AFZ2**			**Tse**			**Wong**		
Predictors	*Estimates*	*CI*	*p*	*Estimates*	*CI*	*p*	*Estimates*	*CI*	*p*	*Estimates*	*CI*	*p*
(Intercept)	0.54	0.43 – 0.66	**<0.001**	0.47	0.18 – 0.75	**0.001**	3.04	2.74 – 3.33	**<0.001**	1.93	1.55 – 2.31	**<0.001**
SSCT Velocity	-0.01	-0.02 – 0.01	0.409	0.25	0.21 – 0.30	**<0.001**	-0.03	-0.06 – -0.01	**0.016**	0.02	-0.03 – 0.08	0.352
Random Effects												
σ^2	0.03			0.04			0.09			0.11		
τ_{00}	0.04 $_{\text{Subject:Study}}$			0.02 $_{\text{Subject}}$			0.15 $_{\text{Subject}}$			0.05 $_{\text{Subject}}$		
	0.00 $_{\text{Study}}$											
ICC	0.55			0.31			0.64			0.30		
N	49 $_{\text{Subject}}$			10 $_{\text{Subject}}$			19 $_{\text{Subject}}$			20 $_{\text{Subject}}$		
	3 $_{\text{Study}}$											
Observations	317			47			190			80		
Marginal R^2 / Conditional R^2	0.002 / 0.554			0.800 / 0.862			0.018 / 0.644			0.011 / 0.308		

Appendix 2.5

Individual study estimates for SSI with FDS velocity as the predictor. Main model results are denoted in the column "SSI" and include the effect of Subject nested within the effect of Study (Subject:Study) as random effects. Individual study behaviours follow in the columns to the right, and use Subject alone as a random effect. Estimates represent the beta-coefficient for the associated predictor variable and are provided with 95% confidence intervals (CI). Significant results are bolded and defined at a level of $p < 0.05$. The intercept represents the estimate for the reference group, and are the following for the predictor variables: FDS Velocity, 0 cm/s. The between group variance for the random effects are provided in the rows denoted by τ_{00}.

	SSI			**AFZ2**			**Kociolek (2016)**			**Tat (2016)**			**Tse (2020)**			**Wong (2019)**		
Predictors	*Estimates*	*CI*	*p*	*Estimates*	*CI*	*p*	*Estimates*	*CI*	*p*	*Estimates*	*CI*	*p*	*Estimates*	*CI*	*p*	*Estimates*	*CI*	*p*
(Intercept)	16.16	6.45 – 25.88	**0.001**	62.30	34.50 – 90.11	**<0.001**	34.30	16.91 – 51.69	**<0.001**	15.04	9.13 – 20.95	**<0.001**	0.40	-4.55 – 5.35	0.874	10.95	1.48 – 20.42	**0.023**
FDS Velocity	1.40	1.14 – 1.66	**<0.001**	-3.26	-6.68 – 0.16	0.062	0.01	-2.80 – 2.82	0.996	1.49	1.20 – 1.77	**<0.001**	1.64	1.26 – 2.03	**<0.001**	1.15	0.22 – 2.08	**0.015**
Random Effects																		
σ^2	66.75			171.43			154.17			55.85			35.00			53.18		
τ_{00}	100.30 $_{\text{Subject:Study}}$ 107.45 $_{\text{Study}}$			289.54 $_{\text{Subject}}$			41.06 $_{\text{Subject}}$			47.56 $_{\text{Subject}}$			34.56 $_{\text{Subject}}$			109.83 $_{\text{Subject}}$		
ICC	0.76			0.63			0.21			0.46			0.50			0.67		
N	73 $_{\text{Subject}}$ 5 $_{\text{Study}}$			10 $_{\text{Subject}}$			16 $_{\text{Subject}}$			8 $_{\text{Subject}}$			19 $_{\text{Subject}}$			20 $_{\text{Subject}}$		
Observations	509			47			48			144			190			80		
Marginal R^2 / Conditional R^2	0.080 / 0.776			0.113 / 0.670			0.000 / 0.210			0.283 / 0.613			0.209 / 0.602			0.038 / 0.686		

Appendix 2.6

Individual study estimates for SSI with SSCT velocity as the predictor. Main model results are denoted in the column "SSI" and include the effect of Subject nested within the effect of Study (Subject:Study) as random effects. Individual study behaviours follow in the columns to the right, and use Subject alone as a random effect. Estimates represent the beta-coefficient for the associated predictor variable and are provided with 95% confidence intervals (CI). Significant results are bolded and defined at a level of $p < 0.05$. The intercept represents the estimate for the reference group, and are the following for the predictor variables: SSCT Velocity, 0 cm/s. The between group variance for the random effects are provided in the rows denoted by τ_{00}.

	SSI			**AFZ2**			**Kociolek (2016)**			**Tat (2016)**			**Tse (2020)**			**Wong (2019)**		
Predictors	*Estimates*	*CI*	*p*	*Estimates*	*CI*	*p*	*Estimates*	*CI*	*p*	*Estimates*	*CI*	*p*	*Estimates*	*CI*	*p*	*Estimates*	*CI*	*p*
(Intercept)	27.60	19.18 – 36.01	**<0.001**	81.87	60.88 – 102.85	**<0.001**	62.18	51.87 – 72.49	**<0.001**	22.94	15.49 – 30.39	**<0.001**	16.87	10.83 – 22.91	**<0.001**	26.23	15.83 – 36.63	**<0.001**
SSCT Velocity	0.13	-0.33 – 0.59	0.574	-7.64	-10.91 – -4.38	**<0.001**	-7.32	-9.82 – -4.81	**<0.001**	1.20	0.55 – 1.84	**<0.001**	0.14	-0.50 – 0.77	0.672	-0.74	-2.05 – 0.58	0.274
Random Effects																		
σ^2	84.66			126.58			83.37			88.49			49.81			59.13		
τ_{00}	92.01 Subject:Study 72.07 Study			206.73 Subject			37.22 Subject			62.17 Subject			30.47 Subject			97.63 Subject		
ICC	0.66			0.62			0.31			0.41			0.38			0.62		
N	73 Subject 5 Study			10 Subject			16 Subject			8 Subject			19 Subject			20 Subject		
Observations	509			47			48			144			190			80		
Marginal R^2 / Conditional R^2	0.000 / 0.660			0.394 / 0.770			0.383 / 0.574			0.060 / 0.448			0.001 / 0.380			0.010 / 0.627		

Appendix 2.7

Individual study estimates for SSI with wrist posture as the predictor. Main model results are denoted in the column "SSI" and include the effect of Subject nested within the effect of Study (Subject:Study) as random effects. Individual study behaviours follow in the columns to the right, and use Subject alone as a random effect. Estimates represent the beta-coefficient for the associated predictor variable and are provided with 95% confidence intervals (CI). Significant results are bolded and defined at a level of $p < 0.05$. The intercept represents the estimate for the reference group, and are the following for the predictor variables: Wrist Posture, Neutral. The between group variance for the random effects are provided in the rows denoted by τ_{00}.

	SSI			**Kociolek (2016)**			**Tat (2016)**		
Predictors	*Estimates*	*CI*	*p*	*Estimates*	*CI*	*p*	*Estimates*	*CI*	*p*
(Intercept)	26.87	21.73 – 32.01	**<0.001**	34.10	27.61 – 40.59	**<0.001**	28.40	23.35 – 33.45	**<0.001**
Wrist Posture (Flexion)	6.96	4.35 – 9.57	**<0.001**	5.91	-1.95 – 13.76	0.141	7.01	3.99 – 10.02	**<0.001**
Wrist Posture (Extension)	-4.32	-9.77 – 1.12	0.120	-5.19	-13.04 – 2.67	0.196			
Random Effects									
σ^2	79.11			128.53			85.36		
τ_{00}	75.15 $_{\text{Subject:Study}}$			47.08 $_{\text{Subject}}$			43.70 $_{\text{Subject}}$		
	41.33 $_{\text{Study}}$								
ICC	0.60			0.27			0.34		
N	127 $_{\text{Subject}}$			16 $_{\text{Subject}}$			8 $_{\text{Subject}}$		
	7 $_{\text{Study}}$								
Observations	579			48			144		
Marginal R^2 / Conditional R^2	0.035 / 0.610			0.107 / 0.346			0.087 / 0.396		

Appendix 2.8

Individual study estimates for MVR with FDS velocity as the predictor. Main model results are denoted in the column "MVR" and include the effect of Subject nested within the effect of Study (Subject:Study) as random effects. Individual study behaviours follow in the columns to the right, and use Subject alone as a random effect. Estimates represent the beta-coefficient for the associated predictor variable and are provided with 95% confidence intervals (CI). Significant results are bolded and defined at a level of $p < 0.05$. The intercept represents the estimate for the reference group, and are the following for the predictor variables: FDS Velocity, 0 cm/s. The between group variance for the random effects are provided in the rows denoted by τ_{00}.

	MVR			**AFZ2**			**Kociolek (2016)**			**Tat (2016)**			**Tse (2020)**			**Wong (2019)**		
Predictors	*Estimates*	*CI*	*p*	*Estimates*	*CI*	*p*	*Estimates*	*CI*	*p*	*Estimates*	*CI*	*p*	*Estimates*	*CI*	*p*	*Estimates*	*CI*	*p*
(Intercept)	92.08	83.02 – 101.15	**<0.001**	82.80	65.99 – 99.61	**<0.001**	69.92	52.74 – 87.10	**<0.001**	93.37	86.99 – 99.76	**<0.001**	100.14	94.39 – 105.88	**<0.001**	96.56	87.98 – 105.13	**<0.001**
FDS Velocity	-1.93	-2.18 – -1.68	**<0.001**	-0.68	-2.71 – 1.35	0.512	-0.91	-3.71 – 1.88	0.521	-2.08	-2.40 – -1.75	**<0.001**	-1.81	-2.25 – -1.37	**<0.001**	-1.67	-2.48 – -0.86	**<0.001**
Random Effects																		
σ^2	63.34			52.16			176.99			70.07			46.99			40.41		
τ_{00}	74.54 Subject:Study 94.00 Study			132.12 Subject			17.16 Subject			53.19 Subject			47.09 Subject			107.34 Subject		
ICC	0.73			0.72			0.09			0.43			0.50			0.73		
N	73 Subject 5 Study			10 Subject			16 Subject			8 Subject			19 Subject			20 Subject		
Observations	509			47			48			144			190			80		
Marginal R^2 / Conditional R^2	0.165 / 0.772			0.014 / 0.721			0.009 / 0.097			0.393 / 0.655			0.191 / 0.596			0.083 / 0.749		

Appendix 2.9

Individual study estimates for MVR with SSCT velocity as the predictor. Main model results are denoted in the column "MVR" and include the effect of Subject nested within the effect of Study (Subject:Study) as random effects. Individual study behaviours follow in the columns to the right, and use Subject alone as a random effect. Estimates represent the beta-coefficient for the associated predictor variable and are provided with 95% confidence intervals (CI). Significant results are bolded and defined at a level of $p < 0.05$. The intercept represents the estimate for the reference group, and are the following for the predictor variables: SSCT Velocity, 0 cm/s. The between group variance for the random effects are provided in the rows denoted by τ_{00}.

	MVR			**AFZ2**			**Kociolek (2016)**			**Tat (2016)**			**Tse (2020)**			**Wong (2019)**		
Predictors	*Estimates*	*CI*	*p*	*Estimates*	*CI*	*p*	*Estimates*	*CI*	*p*	*Estimates*	*CI*	*p*	*Estimates*	*CI*	*p*	*Estimates*	*CI*	*p*
(Intercept)	77.87	70.05 – 85.70	**<0.001**	58.13	44.90 – 71.35	**<0.001**	35.39	24.93 – 45.85	**<0.001**	82.50	73.91 – 91.09	**<0.001**	80.51	73.50 – 87.51	**<0.001**	79.89	69.88 – 89.90	**<0.001**
SSCT Velocity	-0.44	-0.92 – 0.05	0.078	3.43	1.43 – 5.43	**0.001**	7.64	5.08 – 10.21	**<0.001**	-1.69	-2.48 – -0.90	**<0.001**	0.02	-0.71 – 0.75	0.955	0.29	-0.95 – 1.52	0.650
Random Effects																		
σ^2	95.43			42.22			91.41			133.42			64.79			50.53		
τ_{00}	73.26 Subject:Study 59.66 Study			105.13 Subject			28.57 Subject			73.40 Subject			45.59 Subject			112.37 Subject		
ICC	0.58			0.71			0.24			0.35			0.41			0.69		
N	73 Subject 5 Study			10 Subject			16 Subject			8 Subject			19 Subject			20 Subject		
Observations	509			47			48			144			190			80		
Marginal R^2 / Conditional R^2	0.005 / 0.584			0.228 / 0.779			0.405 / 0.547			0.086 / 0.410			0.000 / 0.413			0.002 / 0.690		

Appendix 2.10

Individual study estimates for MVR with wrist posture as the predictor. Main model results are denoted in the column "MVR" and include the effect of Subject nested within the effect of Study (Subject:Study) as random effects. Individual study behaviours follow in the columns to the right, and use Subject alone as a random effect. Estimates represent the beta-coefficient for the associated predictor variable and are provided with 95% confidence intervals (CI). Significant results are bolded and defined at a level of $p < 0.05$. The intercept represents the estimate for the reference group, and are the following for the predictor variables: Wrist Posture, Neutral. The between group variance for the random effects are provided in the rows denoted by τ_{00}.

	MVR			**Kociolek (2016)**			**Tat (2016)**		
Predictors	*Estimates*	*CI*	*p*	*Estimates*	*CI*	*p*	*Estimates*	*CI*	*p*
(Intercept)	76.26	70.63 – 81.90	**<0.001**	66.66	60.27 – 73.04	**<0.001**	73.79	68.41 – 79.18	**<0.001**
Wrist Posture (Flexion)	-8.54	-11.31 – -5.78	**<0.001**	-9.47	-17.67 – -1.27	**0.024**	-7.97	-11.79 – -4.16	**<0.001**
Wrist Posture (Extension)	2.72	-3.05 – 8.48	0.355	2.93	-5.27 – 11.14	0.484			
Random Effects									
σ^2	89.02			140.14			136.35		
τ_{00}	68.98 $_{\text{Subject:Study}}$ 34.27 $_{\text{Study}}$			29.74 $_{\text{Subject}}$			45.26 $_{\text{Subject}}$		
ICC	0.54			0.18			0.25		
N	73 $_{\text{Subject}}$ 5 $_{\text{Study}}$			16 $_{\text{Subject}}$			8 $_{\text{Subject}}$		
Observations	509			48			144		
Marginal R^2 / Conditional R^2	0.054 / 0.562			0.144 / 0.294			0.081 / 0.310		

Appendix 3.1

Least square mean estimates for median nerve blood flow velocity with predictor variables force and wrist posture. Significant results are defined at a level of $p < 0.05$ and highlighted. Levels 0 and 6 refer to 0 N and 6 N of force, respectively.

levels	Estimate	Std. Error	df	t value	lower	upper	Pr(>|t|)
Neutral - Flexion	-0.2492224	0.0706243	694.4975	-3.5288492	-0.3878851	-0.1105597	**0.0004449**
Neutral - Extension	-0.0746299	0.0706223	694.0001	-1.0567470	-0.2132889	0.0640291	0.2909948
Flexion - Extension	0.1745925	0.0668486	690.8445	2.6117616	0.0433418	0.3058432	**0.0092033**
0 - 6	-0.5387022	0.0633489	692.5369	-8.5037406	-0.6630810	-0.4143234	**0.0000000**
Neutral:0 - Flexion:0	-0.2426198	0.0948454	698.3190	-2.5580569	-0.4288361	-0.0564036	**0.0107358**
Neutral:0 - Extension:0	-0.1479446	0.0948396	697.2494	-1.5599465	-0.3341500	0.0382607	0.1192263
Neutral:0 - Neutral:6	-0.5831770	0.1084181	694.5957	-5.3789624	-0.7960435	-0.3703105	**0.0000001**
Neutral:0 - Flexion:6	-0.8390019	0.1032113	694.8841	-8.1289751	-1.0416453	-0.6363586	**0.0000000**
Neutral:0 - Extension:6	-0.5844921	0.1032113	694.8841	-5.6630644	-0.7871355	-0.3818488	**0.0000000**
Flexion:0 - Extension:0	0.0946752	0.0903487	691.9057	1.0478865	-0.0827153	0.2720658	0.2950568
Flexion:0 - Neutral:6	-0.3405571	0.1044676	691.5101	-3.2599307	-0.5456689	-0.1354454	**0.0011690**
Flexion:0 - Flexion:6	-0.5963821	0.0984488	691.6200	-6.0577875	-0.7896765	-0.4030877	**0.0000000**
Flexion:0 - Extension:6	-0.3418723	0.0984488	691.6200	-3.4725886	-0.5351667	-0.1485779	**0.0005476**
Extension:0 - Neutral:6	-0.4352323	0.1044672	691.2295	-4.1662114	-0.6403434	-0.2301213	**0.0000349**
Extension:0 - Flexion:6	-0.6910573	0.0984485	691.3127	-7.0194831	-0.8843512	-0.4977635	**0.0000000**
Extension:0 - Extension:6	-0.4365475	0.0984485	691.3127	-4.4342745	-0.6298414	-0.2432537	**0.0000107**
Neutral:6 - Flexion:6	-0.2558250	0.1040967	689.9971	-2.4575707	-0.4602092	-0.0514407	**0.0142329**
Neutral:6 - Extension:6	-0.0013152	0.1040967	689.9971	-0.0126341	-0.2056994	0.2030691	0.9899234
Flexion:6 - Extension:6	0.2545098	0.0985496	689.9505	2.5825547	0.0610167	0.4480030	**0.0100120**

Appendix 3.2

Individual study estimates for median nerve blood flow velocity (BFV) with CTS status as the predictor. Main model results are denoted in the column "Median Nerve BFV" and include the effect of Subject nested within the effect of Study (Subject:Study) as random effects. Individual study behaviours follow in the columns to the right, and use Subject alone as a random effect. Estimates represent the beta-coefficient for the associated predictor variable and are provided with 95% confidence intervals (CI). Significant results are bolded and defined at a level of $p < 0.05$. The intercept represents the estimate for the reference group, and are the following for the predictor variables: CTS Status, Healthy. The between group variance for the random effects are provided in the rows denoted by τ_{00}.

	Median Nerve BFV			**AFZ1**			**Ehmke**			**Wilson**		
Predictors	*Estimates*	*CI*	*p*	*Estimates*	*CI*	*p*	*Estimates*	*CI*	*p*	*Estimates*	*CI*	*p*
(Intercept)	2.10	1.08 – 3.12	**<0.001**	2.60	2.01 – 3.20	**<0.001**	2.02	1.91 – 2.13	**<0.001**	3.03	2.81 – 3.24	**<0.001**
CTS Status (Possible)	0.27	-0.35 – 0.88	0.398				0.13	-0.02 – 0.29	0.086	0.31	0.01 – 0.62	**0.042**
CTS Status (CTS)	0.51	-1.49 – 2.50	0.620									
CTS Status (Follow-Up)	1.11	-0.91 – 3.12	0.281	0.60	0.07 – 1.13	**0.026**						
Random Effects												
σ^2	0.54			1.37			0.19			0.59		
τ_{00}	0.97 $_{\text{Subject:Study}}$ 0.73 $_{\text{Study}}$			2.50 $_{\text{Subject}}$			0.02 $_{\text{Subject}}$			0.05 $_{\text{Subject}}$		
ICC	0.76			0.65			0.10			0.08		
N	109 $_{\text{Subject}}$ 4 $_{\text{Study}}$			33 $_{\text{Subject}}$			22 $_{\text{Subject}}$			18 $_{\text{Subject}}$		
Observations	812			126			330			180		
Marginal R^2 / Conditional R^2	0.030 / 0.766			0.019 / 0.654			0.021 / 0.120			0.037 / 0.111		

Appendix 3.3

Least square mean estimates for median nerve blood flow velocity with predictor variable CTS Status with levels Healthy, Possible, CTS, and Follow-Up. Significant results are defined at a level of $p < 0.05$ and highlighted.

levels	Estimate	Std. Error	df	t value	lower	upper	Pr(>|t|)
Healthy - Possible	-0.2664111	0.3154575	87.506799	-0.8445231	-0.8933658	0.3605436	0.4006801
Healthy - CTS	-0.5060625	1.0195664	1.946982	-0.4963507	-5.0093906	3.9972655	0.6700063
Healthy - Follow-Up	-1.1063903	1.0268747	2.003410	-1.0774345	-5.5174775	3.3046968	0.3938152
Possible - CTS	-0.2396514	1.0360008	2.075125	-0.2313235	-4.5460737	4.0667709	0.8378820
Possible - Follow-Up	-0.8399792	1.0431941	2.133358	-0.8051994	-5.0700393	3.3900809	0.5006044
CTS - Follow-Up	-0.6003278	0.1700284	768.567056	-3.5307496	-0.9341030	-0.2665526	**0.0004391**

Appendix 3.4

Individual study estimates for median nerve blood flow velocity (BFV) with CTS status as the predictor, with CTS separated into its corresponding severities. Main model results are denoted in the column "Median Nerve BFV" and include the effect of Subject nested within the effect of Study (Subject:Study) as random effects. Individual study behaviours follow in the columns to the right, and use Subject alone as a random effect. Estimates represent the beta-coefficient for the associated predictor variable and are provided with 95% confidence intervals (CI). Significant results are bolded and defined at a level of $p < 0.05$. The intercept represents the estimate for the reference group, and are the following for the predictor variables: CTS Status 2, Healthy. The between group variance for the random effects are provided in the rows denoted by τ_{00}.

	Median Nerve BFV			**AFZ1**			**Ehmke**			**Wilson**		
Predictors	*Estimates*	*CI*	*p*	*Estimates*	*CI*	*p*	*Estimates*	*CI*	*p*	*Estimates*	*CI*	*p*
(Intercept)	2.10	1.08 – 3.12	**<0.001**	2.92	2.09 – 3.75	**<0.001**	2.02	1.91 – 2.13	**<0.001**	3.03	2.81 – 3.24	**<0.001**
CTS Status 2 (Possible)	0.27	-0.35 – 0.88	0.396				0.13	-0.02 – 0.29	0.086	0.31	0.01 – 0.62	**0.042**
CTS Status 2 (Mild)	0.82	-1.21 – 2.86	0.426									
CTS Status 2 (Moderate)	0.55	-1.48 – 2.58	0.595	-0.27	-1.25 – 0.71	0.588						
CTS Status 2 (Severe)	-0.01	-2.07 – 2.05	0.994	-0.83	-2.03 – 0.36	0.173						
CTS Status 2 (Follow-Up)	1.16	-0.85 – 3.18	0.257	0.34	-0.41 – 1.10	0.371						
Random Effects												
σ^2	0.54			1.37			0.19			0.59		
τ_{00}	0.96 $_{\text{Subject:Study}}$ 0.73 $_{\text{Study}}$			2.49 $_{\text{Subject}}$			0.02 $_{\text{Subject}}$			0.05 $_{\text{Subject}}$		
ICC	0.76			0.64			0.10			0.08		
N	109 $_{\text{Subject}}$ 4 $_{\text{Study}}$			33 $_{\text{Subject}}$			22 $_{\text{Subject}}$			18 $_{\text{Subject}}$		
Observations	812			126			330			180		
Marginal R^2 / Conditional R^2	0.037 / 0.766			0.042 / 0.660			0.021 / 0.120			0.037 / 0.111		

Appendix 3.5

Least square mean estimates for median nerve blood flow velocity with predictor variable CTS Status with levels Healthy, Possible, Mild, Moderate, Severe, and Follow-Up. Significant results are defined at a level of $p < 0.05$ and highlighted.

levels	Estimate	Std. Error	df	t value	lower	upper	Pr(>|t|)
Healthy - Possible	-0.2655525	0.3129256	86.404214	-0.8486120	-0.8875865	0.3564816	0.3984421
Healthy - Mild	-0.8246341	1.0362706	2.078763	-0.7957710	-5.1253039	3.4760357	0.5068585
Healthy - Moderate	-0.5505124	1.0344853	2.064474	-0.5321607	-4.8709534	3.7699287	0.6463484
Healthy - Severe	0.0075988	1.0515759	2.204319	0.0072261	-4.1379109	4.1531085	0.9948359
Healthy - Follow-Up	-1.1645426	1.0273548	2.008130	-1.1335350	-5.5677873	3.2387021	0.3741721
Possible - Mild	-0.5590816	1.0521825	2.208903	-0.5313542	-4.6997315	3.5815682	0.6438107
Possible - Moderate	-0.2849599	1.0504242	2.194179	-0.2712808	-4.4421090	3.8721891	0.8095946
Possible - Severe	0.2731512	1.0672596	2.338197	0.2559370	-3.7376125	4.2839150	0.8187965
Possible - Follow-Up	-0.8989901	1.0434027	2.136110	-0.8615946	-5.1251027	3.3271225	0.4746806
Mild - Moderate	0.2741217	0.3128162	615.429573	0.8763028	-0.3401949	0.8884383	0.3812074
Mild - Severe	0.8322329	0.3815249	413.995623	2.1813330	0.0822653	1.5822004	**0.0297207**
Mild - Follow-Up	-0.3399085	0.2413008	778.959581	-1.4086507	-0.8135853	0.1337683	0.1593375
Moderate - Severe	0.5581112	0.3771479	413.215742	1.4798205	-0.1832565	1.2994789	0.1396831
Moderate - Follow-Up	-0.6140302	0.2354677	790.391532	-2.6077042	-1.0762463	-0.1518141	**0.0092871**
Severe - Follow-Up	-1.1721414	0.3328696	480.875358	-3.5213228	-1.8262000	-0.5180827	**0.0004703**

Appendix 3.6

Individual study estimates for median nerve blood flow velocity (BFV) with presence of CTS symptoms as the predictor. Main model results are denoted in the column "Median Nerve BFV" and include the effect of Subject nested within the effect of Study (Subject:Study) as random effects. Individual study behaviours follow in the columns to the right, and use Subject alone as a random effect. Estimates represent the beta-coefficient for the associated predictor variable and are provided with 95% confidence intervals (CI). Significant results are bolded and defined at a level of $p < 0.05$. The intercept represents the estimate for the reference group, and are the following for the predictor variables: Symptoms, No. The between group variance for the random effects are provided in the rows denoted by τ_{00}.

	Median Nerve BFV			**Ehmke**			**Wilson**		
Predictors	*Estimates*	*CI*	*p*	*Estimates*	*CI*	*p*	*Estimates*	*CI*	*p*
(Intercept)	2.17	1.39 – 2.95	**<0.001**	2.02	1.91 – 2.13	**<0.001**	3.03	2.81 – 3.24	**<0.001**
Symptoms (Yes)	0.32	-0.27 – 0.91	0.291	0.13	-0.02 – 0.29	0.086	0.31	0.01 – 0.62	**0.042**
Random Effects									
σ^2	0.55			0.19			0.59		
τ_{00}	0.94 $_{\text{Subject:Study}}$			0.02 $_{\text{Subject}}$			0.05 $_{\text{Subject}}$		
	0.50 $_{\text{Study}}$								
ICC	0.72			0.10			0.08		
N	109 $_{\text{Subject}}$			22 $_{\text{Subject}}$			18 $_{\text{Subject}}$		
	4 $_{\text{Study}}$								
Observations	812			330			180		
Marginal R^2 / Conditional R^2	0.012 / 0.727			0.021 / 0.120			0.037 / 0.111		

Appendix 4.1

Individual study estimates for FDS displacement model with altered blood flow as the predictor. Main model results are denoted in the column "FDS Displacement" and include the effect of Subject nested within Study (Subject:Study) as random effects. Individual study behaviours follow in the columns to the right, and use Subject alone as a random effect. Estimates represent the beta-coefficient for the associated predictor variable and are provided with 95% confidence intervals (CI). Significant results are bolded and defined at a level of $p < 0.05$. The intercept represents the estimate for the reference group, and are the following for the predictor variables: Altered Blood Flow, No. The between group variance for the random effects are provided in the rows denoted by τ_{00}.

	FDS Displacement			**AFZ2**			**Tse (2020)**			**Wong (2019)**		
Predictors	*Estimates*	*CI*	*p*	*Estimates*	*CI*	*p*	*Estimates*	*CI*	*p*	*Estimates*	*CI*	*p*
(Intercept)	2.32	1.85 – 2.78	**<0.001**	2.07	1.75 – 2.39	**<0.001**	2.77	2.60 – 2.94	**<0.001**	2.16	2.01 – 2.30	**<0.001**
Altered Blood Flow (Yes)	-0.12	-0.20 – -0.04	**0.003**	-0.20	-0.43 – 0.03	0.082	-0.10	-0.20 – 0.01	0.078	-0.11	-0.25 – 0.03	0.115
Random Effects												
σ^2	0.09			0.11			0.09			0.10		
τ_{00}	0.11 $_{\text{Subject:Study}}$			0.16 $_{\text{Subject}}$			0.13 $_{\text{Subject}}$			0.06 $_{\text{Subject}}$		
	0.16 $_{\text{Study}}$											
ICC	0.74			0.60			0.59			0.36		
N	49 $_{\text{Subject}}$			10 $_{\text{Subject}}$			19 $_{\text{Subject}}$			20 $_{\text{Subject}}$		
	3 $_{\text{Study}}$											
Observations	317			47			190			80		
Marginal R^2 / Conditional R^2	0.009 / 0.743			0.026 / 0.609			0.007 / 0.594			0.020 / 0.369		

Appendix 4.2

Individual study estimates for FDS displacement model with altered blood flow type as the predictor. Main model results are denoted in the column "FDS Displacement" and include the effect of Subject nested within Study (Subject:Study) as random effects. Individual study behaviours follow in the columns to the right, and use Subject alone as a random effect. Estimates represent the beta-coefficient for the associated predictor variable and are provided with 95% confidence intervals (CI). Significant results are bolded and defined at a level of $p < 0.05$. The intercept represents the estimate for the reference group, and are the following for the predictor variables: Altered Blood Flow Type, None. The between group variance for the random effects are provided in the rows denoted by τ_{00}.

	FDS Displacement			**AFZ2**			**Tse (2020)**			**Wong (2019)**		
Predictors	*Estimates*	*CI*	*p*	*Estimates*	*CI*	*p*	*Estimates*	*CI*	*p*	*Estimates*	*CI*	*p*
(Intercept)	2.33	1.88 – 2.78	**<0.001**	2.07	1.75 – 2.39	**<0.001**	2.77	2.60 – 2.94	**<0.001**	2.16	2.01 – 2.30	**<0.001**
Altered Blood Flow Type (Subdiastolic)	-0.14	-0.26 – -0.03	**0.013**	-0.20	-0.43 – 0.03	0.082				-0.11	-0.25 – 0.03	0.115
Altered Blood Flow Type (Supradiastolic)	-0.09	-0.20 – 0.02	0.092				-0.10	-0.20 – 0.01	0.078			
Random Effects												
σ^2	0.09			0.11			0.09			0.10		
τ_{00}	0.11 $_{\text{Subject:Study}}$ 0.15 $_{\text{Study}}$			0.16 $_{\text{Subject}}$			0.13 $_{\text{Subject}}$			0.06 $_{\text{Subject}}$		
ICC	0.73			0.60			0.59			0.36		
N	49 $_{\text{Subject}}$ 3 $_{\text{Study}}$			10 $_{\text{Subject}}$			19 $_{\text{Subject}}$			20 $_{\text{Subject}}$		
Observations	317			47			190			80		
Marginal R^2 / Conditional R^2	0.011 / 0.736			0.026 / 0.609			0.007 / 0.594			0.020 / 0.369		

Appendix 4.3

Individual study estimates for SSCT displacement model with altered blood flow as the predictor. Main model results are denoted in the column "SSCT Displacement" and include the effect of Subject nested within Study (Subject:Study) as random effects. Individual study behaviours follow in the columns to the right, and use Subject alone as a random effect. Estimates represent the beta-coefficient for the associated predictor variable and are provided with 95% confidence intervals (CI). Significant results are bolded and defined at a level of $p < 0.05$. The intercept represents the estimate for the reference group, and are the following for the predictor variables: Altered Blood Flow, No. The between group variance for the random effects are provided in the rows denoted by τ_{00}.

	SSCT Displacement			**AFZ2**			**Tse (2020)**			**Wong (2019)**		
Predictors	*Estimates*	*CI*	*p*	*Estimates*	*CI*	*p*	*Estimates*	*CI*	*p*	*Estimates*	*CI*	*p*
(Intercept)	2.17	1.77 – 2.56	**<0.001**	2.38	2.06 – 2.70	**<0.001**	2.32	2.18 – 2.47	**<0.001**	1.78	1.62 – 1.94	**<0.001**
Altered Blood Flow (Yes)	-0.12	-0.20 – -0.03	**0.009**	-0.07	-0.28 – 0.15	0.559	-0.12	-0.25 – -0.00	**0.046**	-0.13	-0.28 – 0.03	0.109
Random Effects												
σ^2	0.12			0.10			0.12			0.13		
τ_{00}	0.10 $_{\text{Subject:Study}}$			0.17 $_{\text{Subject}}$			0.09 $_{\text{Subject}}$			0.07 $_{\text{Subject}}$		
	0.11 $_{\text{Study}}$											
ICC	0.64			0.64			0.43			0.34		
N	49 $_{\text{Subject}}$			10 $_{\text{Subject}}$			19 $_{\text{Subject}}$			20 $_{\text{Subject}}$		
	3 $_{\text{Study}}$											
Observations	317			47			190			80		
Marginal R^2 / Conditional R^2	0.010 / 0.647			0.003 / 0.636			0.012 / 0.434			0.021 / 0.354		

Appendix 4.4

Individual study estimates for SSCT displacement model with altered blood flow type as the predictor. Main model results are denoted in the column "SSCT Displacement" and include the effect of Subject nested within Study (Subject:Study) as random effects. Individual study behaviours follow in the columns to the right, and use Subject alone as a random effect. Estimates represent the beta-coefficient for the associated predictor variable and are provided with 95% confidence intervals (CI). Significant results are bolded and defined at a level of $p < 0.05$. The intercept represents the estimate for the reference group, and are the following for the predictor variables: Altered Blood Flow Type, None. The between group variance for the random effects are provided in the rows denoted by τ_{00}.

	SSCT Displacement			**AFZ2**			**Tse (2020)**			**Wong (2019)**		
Predictors	*Estimates*	*CI*	*p*	*Estimates*	*CI*	*p*	*Estimates*	*CI*	*p*	*Estimates*	*CI*	*p*
(Intercept)	2.17	1.77 – 2.56	**<0.001**	2.38	2.06 – 2.70	**<0.001**	2.32	2.18 – 2.47	**<0.001**	1.78	1.62 – 1.94	**<0.001**
Altered Blood Flow Type (Subdiastolic)	-0.11	-0.24 – 0.02	0.089	-0.07	-0.28 – 0.15	0.559				-0.13	-0.28 – 0.03	0.109
Altered Blood Flow Type (Supradiastolic)	-0.12	-0.24 – -0.00	**0.047**				-0.12	-0.25 – -0.00	**0.046**			
Random Effects												
σ^2	0.12			0.10			0.12			0.13		
τ_{00}	0.09 $_{\text{Subject:Study}}$ 0.11 $_{\text{Study}}$			0.17 $_{\text{Subject}}$			0.09 $_{\text{Subject}}$			0.07 $_{\text{Subject}}$		
ICC	0.64			0.64			0.43			0.34		
N	49 $_{\text{Subject}}$ 3 $_{\text{Study}}$			10 $_{\text{Subject}}$			19 $_{\text{Subject}}$			20 $_{\text{Subject}}$		
Observations	317			47			190			80		
Marginal R^2 / Conditional R^2	0.009 / 0.646			0.003 / 0.636			0.012 / 0.434			0.021 / 0.354		

Appendix 4.5

Individual study estimates for relative displacement model with altered blood flow as the predictor. Main model results are denoted in the column "Relative Displacement" and include the effect of Subject nested within Study (Subject:Study) as random effects. Individual study behaviours follow in the columns to the right, and use Subject alone as a random effect. Estimates represent the beta-coefficient for the associated predictor variable and are provided with 95% confidence intervals (CI). Significant results are bolded and defined at a level of $p < 0.05$. The intercept represents the estimate for the reference group, and are the following for the predictor variables: Altered Blood Flow Type, None. The between group variance for the random effects are provided in the rows denoted by τ_{00}.

	Relative Displacement			**AFZ2**			**Tse (2020)**			**Wong (2019)**		
Predictors	*Estimates*	*CI*	*p*	*Estimates*	*CI*	*p*	*Estimates*	*CI*	*p*	*Estimates*	*CI*	*p*
(Intercept)	0.50	0.43 – 0.57	**<0.001**	0.54	0.38 – 0.70	**<0.001**	0.50	0.42 – 0.58	**<0.001**	0.46	0.34 – 0.57	**<0.001**
Altered Blood Flow (Yes)	0.02	0.03 – 0.06	0.504	0.08	0.05 – 0.20	0.219	0.01	0.05 – 0.08	0.725	-0.01	0.08 – 0.06	0.757
Random Effects												
σ^2	0.03			0.03			0.03			0.02		
τ_{00}	0.04 $_{\text{Subject:Study}}$ 0.00 $_{\text{Study}}$			0.03 $_{\text{Subject}}$			0.03 $_{\text{Subject}}$			0.05 $_{\text{Subject}}$		
ICC	0.56			0.52			0.46			0.70		
N	49 $_{\text{Subject}}$ 3 $_{\text{Study}}$			10 $_{\text{Subject}}$			19 $_{\text{Subject}}$			20 $_{\text{Subject}}$		
Observations	317			47			190			80		
Marginal R^2 /Conditional R^2	0.001 / 0.561			0.015 / 0.531			0.000 / 0.465			0.000 / 0.702		

Appendix 4.6

Individual study estimates for relative displacement model with altered blood flow type as the predictor. Main model results are denoted in the column "Relative Displacement" and include the effect of Subject nested within Study (Subject:Study) as random effects. Individual study behaviours follow in the columns to the right, and use Subject alone as a random effect. Estimates represent the beta-coefficient for the associated predictor variable and are provided with 95% confidence intervals (CI). Significant results are bolded and defined at a level of $p < 0.05$. The intercept represents the estimate for the reference group, and are the following for the predictor variables: Altered Blood Flow Type, None. The between group variance for the random effects are provided in the rows denoted by τ_{00}.

	Relative Displacement			**AFZ2**			**Tse (2020)**			**Wong (2019)**		
Predictors	*Estimates*	*CI*	*p*	*Estimates*	*CI*	*p*	*Estimates*	*CI*	*p*	*Estimates*	*CI*	*p*
(Intercept)	0.50	0.42 – 0.57	**<0.001**	0.54	0.38 – 0.70	**<0.001**	0.50	0.42 – 0.58	**<0.001**	0.46	0.34 – 0.57	**<0.001**
Altered Blood Flow Type (Subdiastolic)	0.02	-0.04 – 0.08	0.564	0.08	-0.05 – 0.20	0.219				-0.01	-0.08 – 0.06	0.757
Altered Blood Flow Type (Supradiastolic)	0.01	-0.05 – 0.08	0.708				0.01	-0.05 – 0.08	0.725			
Random Effects												
σ^2	0.03			0.03			0.03			0.02		
τ_{00}	0.04 $_{\text{Subject:Study}}$ 0.00 $_{\text{Study}}$			0.03 $_{\text{Subject}}$			0.03 $_{\text{Subject}}$			0.05 $_{\text{Subject}}$		
ICC	0.56			0.52			0.46			0.70		
N	49 $_{\text{Subject}}$ 3 $_{\text{Study}}$			10 $_{\text{Subject}}$			19 $_{\text{Subject}}$			20 $_{\text{Subject}}$		
Observations	317			47			190			80		
Marginal R^2 / Conditional R^2	0.001 / 0.561			0.015 / 0.531			0.000 / 0.465			0.000 / 0.702		

Appendix 4.7

Individual study estimates for SSI with altered blood flow as the predictor. Main model results are denoted in the column "SSI" and include the effect of Subject nested within Study (Subject:Study) as random effects. Individual study behaviours follow in the columns to the right, and use Subject alone as a random effect. Estimates represent the beta-coefficient for the associated predictor variable and are provided with 95% confidence intervals (CI). Significant results are bolded and defined at a level of $p < 0.05$. The intercept represents the estimate for the reference group, and are the following for the predictor variables: Altered Blood Flow, None. The between group variance for the random effects are provided in the rows denoted by τ_{00}.

	SSI			**AFZ2**			**Tse (2020)**			**Wong (2019)**		
Predictors	*Estimates*	*CI*	*p*	*Estimates*	*CI*	*p*	*Estimates*	*CI*	*p*	*Estimates*	*CI*	*p*
(Intercept)	24.47	13.04 – 35.90	**<0.001**	30.66	17.40 – 43.93	**<0.001**	17.89	15.21 – 20.56	**<0.001**	20.62	15.47 – 25.76	**<0.001**
Altered Blood Flow (Yes)	2.04	-0.10 – 4.18	0.062	9.48	0.38 – 18.57	**0.041**	0.79	-1.72 – 3.30	0.536	0.84	-2.50 – 4.19	0.621
Random Effects												
σ^2	69.57			168.61			49.95			58.28		
τ_{00}	110.35 $_{\text{Subject:Study}}$ 92.90 $_{\text{Study}}$			289.29 $_{\text{Subject}}$			29.13 $_{\text{Subject}}$			108.51 $_{\text{Subject}}$		
ICC	0.75			0.63			0.37			0.65		
N	49 $_{\text{Subject}}$ 3 $_{\text{Study}}$			10 $_{\text{Subject}}$			19 $_{\text{Subject}}$			20 $_{\text{Subject}}$		
Observations	317			47			190			80		
Marginal R^2 / Conditional R^2	0.004 / 0.746			0.032 / 0.644			0.001 / 0.369			0.001 / 0.651		

Appendix 4.8

Individual study estimates for SSI model with altered blood flow type as the predictor. Main model results are denoted in the column "SSI" and include the effect of Subject nested within Study (Subject:Study) as random effects. Individual study behaviours follow in the columns to the right, and use Subject alone as a random effect. Estimates represent the beta-coefficient for the associated predictor variable and are provided with 95% confidence intervals (CI). Significant results are bolded and defined at a level of $p < 0.05$. The intercept represents the estimate for the reference group, and are the following for the predictor variables: Altered Blood Flow Type, None. The between group variance for the random effects are provided in the rows denoted by τ_{00}.

	SSI			**AFZ2**			**Tse (2020)**			**Wong (2019)**		
Predictors	*Estimates*	*CI*	*p*	*Estimates*	*CI*	*p*	*Estimates*	*CI*	*p*	*Estimates*	*CI*	*p*
(Intercept)	23.95	13.10 – 34.79	**<0.001**	30.66	17.40 – 43.93	**<0.001**	17.89	15.21 – 20.56	**<0.001**	20.62	15.47 – 25.76	**<0.001**
Altered Blood Flow Type (Subdiastolic)	3.44	0.36 – 6.52	**0.029**	9.48	0.38 – 18.57	**0.041**				0.84	-2.50 – 4.19	0.621
Altered Blood Flow Type (Supradiastolic)	0.76	-2.20 – 3.72	0.615				0.79	-1.72 – 3.30	0.536			
Random Effects												
σ^2	69.49			168.61			49.95			58.28		
τ_{00}	110.43 $_{\text{Subject:Study}}$ 82.24 $_{\text{Study}}$			289.29 $_{\text{Subject}}$			29.13 $_{\text{Subject}}$			108.51 $_{\text{Subject}}$		
ICC	0.73			0.63			0.37			0.65		
N	49 $_{\text{Subject}}$ 3 $_{\text{Study}}$			10 $_{\text{Subject}}$			19 $_{\text{Subject}}$			20 $_{\text{Subject}}$		
Observations	317			47			190			80		
Marginal R^2 / Conditional R^2	0.008 / 0.737			0.032 / 0.644			0.001 / 0.369			0.001 / 0.651		

Appendix 4.9

Individual study estimates for MVR model with altered blood flow type as the predictor. Main model results are denoted in the column "MVR" and include the effect of Subject nested within Study (Subject:Study) as random effects. Individual study behaviours follow in the columns to the right, and use Subject alone as a random effect. Estimates represent the beta-coefficient for the associated predictor variable and are provided with 95% confidence intervals (CI). Significant results are bolded and defined at a level of $p < 0.05$. The intercept represents the estimate for the reference group, and are the following for the predictor variables: Altered Blood Flow, None. The between group variance for the random effects are provided in the rows denoted by τ_{00}.

	MVR			**AFZ2**			**Tse (2020)**			**Wong (2019)**		
Predictors	*Estimates*	*CI*	*p*	*Estimates*	*CI*	*p*	*Estimates*	*CI*	*p*	*Estimates*	*CI*	*p*
(Intercept)	81.29	78.44 – 84.14	**<0.001**	83.75	75.81 – 91.70	**<0.001**	80.80	77.51 – 84.09	**<0.001**	82.26	77.07 – 87.46	**<0.001**
Altered Blood Flow (Yes)	-1.62	-3.57 – 0.33	0.103	-7.55	-11.98 – -3.12	**0.001**	-0.58	-3.44 – 2.28	0.692	-0.70	-3.81 – 2.40	0.656
Random Effects												
σ^2	59.00			40.23			64.74			50.14		
τ_{00}	83.77 $_{\text{Subject:Study}}$ 0.00 $_{\text{Study}}$			124.24 $_{\text{Subject}}$			45.54 $_{\text{Subject}}$			115.57 $_{\text{Subject}}$		
ICC				0.76			0.41			0.70		
N	49 $_{\text{Subject}}$ 3 $_{\text{Study}}$			10 $_{\text{Subject}}$			19 $_{\text{Subject}}$			20 $_{\text{Subject}}$		
Observations	318			48			190			80		
Marginal R^2 / Conditional R^2	0.010 / NA			0.055 / 0.769			0.000 / 0.413			0.001 / 0.698		

Appendix 4.10

Individual study estimates for MVR model with altered blood flow type as the predictor. Main model results are denoted in the column "MVR" and include the effect of Subject nested within Study (Subject:Study) as random effects. Individual study behaviours follow in the columns to the right, and use Subject alone as a random effect. Estimates represent the beta-coefficient for the associated predictor variable and are provided with 95% confidence intervals (CI). Significant results are bolded and defined at a level of $p < 0.05$. The intercept represents the estimate for the reference group, and are the following for the predictor variables: Altered Blood Flow Type, None. The between group variance for the random effects are provided in the rows denoted by τ_{00}.

	MVR			**AFZ2**			**Tse (2020)**			**Wong (2019)**		
Predictors	*Estimates*	*CI*	*p*	*Estimates*	*CI*	*p*	*Estimates*	*CI*	*p*	*Estimates*	*CI*	*p*
(Intercept)	81.55	78.65 – 84.45	**<0.001**	83.75	75.81 – 91.70	**<0.001**	80.80	77.51 – 84.09	**<0.001**	82.26	77.07 – 87.46	**<0.001**
Altered Blood Flow Type (Subdiastolic)	-2.59	-5.30 – 0.12	0.061	-7.55	-11.98 – -3.12	**0.001**				-0.70	-3.81 – 2.40	0.656
Altered Blood Flow Type (Supradiastolic)	-0.64	-3.36 – 2.08	0.645				-0.58	-3.44 – 2.28	0.692			
Random Effects												
σ^2	58.98			40.23			64.74			50.14		
τ_{00}	83.96 $_{\text{Subject:Study}}$ 0.00 $_{\text{Study}}$			124.24 $_{\text{Subject}}$			45.54 $_{\text{Subject}}$			115.57 $_{\text{Subject}}$		
ICC	0.59			0.76			0.41			0.70		
N	49 $_{\text{Subject}}$ 3 $_{\text{Study}}$			10 $_{\text{Subject}}$			19 $_{\text{Subject}}$			20 $_{\text{Subject}}$		
Observations	318			48			190			80		
Marginal R^2 / Conditional R^2	0.008 / 0.591			0.055 / 0.769			0.000 / 0.413			0.001 / 0.698		

Appendix 4.11

Individual study estimates for median nerve blood flow velocity (BFV) with CTS status as the predictor including individuals with altered blood flow. Main model results are denoted in the column "Median Nerve BFV" and include the effect of Subject nested within the effect of Study (Subject:Study) as random effects. Individual study behaviours follow in the columns to the right, and use Subject alone as a random effect. Estimates represent the beta-coefficient for the associated predictor variable and are provided with 95% confidence intervals (CI). Significant results are bolded and defined at a level of $p < 0.05$. The intercept represents the estimate for the reference group, and are the following for the predictor variables: CTS Status, Healthy. The between group variance for the random effects are provided in the rows denoted by τ_{00}.

	Median Nerve BFV			**AFZ1**			**AFZ2**			**Ehmke**			**Wilson**		
Predictors	*Estimates*	*CI*	*p*	*Estimates*	*CI*	*p*	*Estimates*	*CI*	*p*	*Estimates*	*CI*	*p*	*Estimates*	*CI*	*p*
(Intercept)	1.98	1.54 – 2.43	**<0.001**	2.92	2.09 – 3.75	**<0.001**	1.98	1.62 – 2.34	**<0.001**	2.02	1.91 – 2.13	**<0.001**	3.03	2.81 – 3.24	**<0.001**
CTS Status Healthy-T1)	-0.91	-1.27 – -0.55	**<0.001**				-0.91	-1.26 – -0.55	**<0.001**						
CTS Status (Healthy-T2)	-0.68	-1.04 – -0.32	**<0.001**				-0.68	-1.03 – -0.33	**<0.001**						
CTS Status (Healthy-T3)	-0.85	-1.22 – -0.49	**<0.001**				-0.85	-1.21 – -0.50	**<0.001**						
CTS Status (Healthy-T4)	-0.91	-1.27 – -0.56	**<0.001**				-0.91	-1.26 – -0.56	**<0.001**						
CTS Status (Possible)	0.22	-0.45 – 0.88	0.524							0.13	-0.02 – 0.29	0.086	0.31	0.01 – 0.62	**0.042**
CTS Status (Mild)	0.29	-0.69 – 1.27	0.562												
CTS Status (Moderate)	0.37	-0.56 – 1.31	0.434	-0.27	-1.25 – 0.71	0.588									
CTS Status (Severe)	0.45	-0.60 – 1.50	0.402	-0.83	-2.03 – 0.36	0.173									
CTS Status (Follow-Up)	1.47	0.56 – 2.38	**0.002**	0.34	-0.41 – 1.10	0.371									
Random Effects															
σ^2	0.62			1.37			0.57			0.19			0.59		
τ_{00}	0.95 $_{\text{Subject:Study}}$ 0.06 $_{\text{Study}}$			2.49 $_{\text{Subject}}$			0.64 $_{\text{Subject}}$			0.02 $_{\text{Subject}}$			0.05 $_{\text{Subject}}$		
ICC	0.62			0.64			0.53			0.10			0.08		
N	107 $_{\text{Subject}}$ 4 $_{\text{Study}}$			33 $_{\text{Subject}}$			36 $_{\text{Subject}}$			22 $_{\text{Subject}}$			18 $_{\text{Subject}}$		
Observations	280			126			176			330			180		
Marginal R^2 / Conditional R^2	0.191 / 0.692			0.042 / 0.660			0.092 / 0.570			0.021 / 0.120			0.037 / 0.111		

Appendix 4.12

Least square mean estimates for median nerve blood flow velocity with predictor variable CTS Status with levels Healthy, Possible, CTS, and Follow-Up. Significant results are defined at a level of $p < 0.05$ and highlighted.

levels	Estimate	Std. Error	df	t value	lower	upper	Pr(>|t|)
Healthy - Healthy-T1	0.9078761	0.1830675	147.577403	4.9592429	0.5461038	1.2696483	**0.0000019**
Healthy - Healthy-T2	0.6793534	0.1831462	147.710765	3.7093507	0.3174283	1.0412785	**0.0002935**
Healthy - Healthy-T3	0.8548878	0.1848617	148.381761	4.6244721	0.4895862	1.2201894	**0.0000081**
Healthy - Healthy-T4	0.9138323	0.1814316	146.910783	5.0367857	0.5552792	1.2723854	**0.0000014**
Healthy - Possible	-0.2160296	0.3387011	39.085400	-0.6378180	-0.9010694	0.4690101	0.5273114
Healthy - Mild	-0.2898477	0.5002433	3.721733	-0.5794136	-1.7206747	1.1409792	0.5955601
Healthy - Moderate	-0.3745540	0.4784450	3.115853	-0.7828570	-1.8656476	1.1165396	0.4888763
Healthy - Severe	-0.4502861	0.5372434	4.942991	-0.8381418	-1.8361188	0.9355465	0.4405840
Healthy - Follow-Up	-1.4677067	0.4646900	2.772032	-3.1584643	-3.0177982	0.0823848	0.0567195
Healthy-T1 - Healthy-T2	-0.2285227	0.1886303	155.753050	-1.2114844	-0.6011265	0.1440811	0.2275446
Healthy-T1 - Healthy-T3	-0.0529883	0.1903168	155.963119	-0.2784214	-0.4289194	0.3229428	0.7810577
Healthy-T1 - Healthy-T4	0.0059563	0.1869412	155.415891	0.0318617	-0.3633172	0.3752297	0.9746232
Healthy-T1 - Possible	-1.1239057	0.3697764	27.274102	-3.0394197	-1.8822676	-0.3655438	**0.0051811**
Healthy-T1 - Mild	-1.1977238	0.5167008	3.948640	-2.3180218	-2.6397044	0.2442568	0.0821687
Healthy-T1 - Moderate	-1.2824301	0.4956269	3.344569	-2.5874906	-2.7716754	0.2068152	0.0727777
Healthy-T1 - Severe	-1.3581622	0.5526001	5.158368	-2.4577666	-2.7656486	0.0493241	0.0558763
Healthy-T1 - Follow-Up	-2.3755828	0.4823621	2.999245	-4.9248949	-3.9108931	-0.8402724	**0.0160531**
Healthy-T2 - Healthy-T3	0.1755344	0.1896404	155.421348	0.9256175	-0.1990707	0.5501396	0.3560798
Healthy-T2 - Healthy-T4	0.2344790	0.1870182	155.538629	1.2537760	-0.1349444	0.6039023	0.2118046
Healthy-T2 - Possible	-0.8953830	0.3698154	27.284641	-2.4211622	-1.6538112	-0.1369547	**0.0223895**
Healthy-T2 - Mild	-0.9692011	0.5167287	3.949489	-1.8756478	-2.4111353	0.4727331	0.1348664
Healthy-T2 - Moderate	-1.0539074	0.4956560	3.345352	-2.1262879	-2.5430683	0.4352535	0.1140710
Healthy-T2 - Severe	-1.1296395	0.5526262	5.159334	-2.0441294	-2.5371159	0.2778369	0.0946172
Healthy-T2 - Follow-Up	-2.1470600	0.4823920	2.999986	-4.4508617	-3.6822506	-0.6118695	**0.0211036**
Healthy-T3 - Healthy-T4	0.0589445	0.1886986	155.739166	0.3123740	-0.3137943	0.4316833	0.7551742

levels	Estimate	Std. Error	df	t value	lower	upper	Pr(>|t|)
Healthy-T3 - Possible	-1.0709174	0.3706680	27.530135	-2.8891556	-1.8307806	-0.3110543	**0.0074448**
Healthy-T3 - Mild	-1.1447355	0.5173393	3.968085	-2.2127366	-2.5856672	0.2961962	0.0918913
Healthy-T3 - Moderate	-1.2294418	0.4962925	3.362495	-2.4772526	-2.7167765	0.2578928	**0.0803620**
Healthy-T3 - Severe	-1.3051739	0.5531971	5.180535	-2.3593288	-2.7124356	0.1020877	0.0630224
Healthy-T3 - Follow-Up	-2.3225945	0.4830459	3.016209	-4.8082270	-3.8551991	-0.7899899	**0.0169178**
Healthy-T4 - Possible	-1.1298620	0.3689693	27.043062	-3.0622114	-1.8868680	-0.3728559	**0.0049250**
Healthy-T4 - Mild	-1.2036801	0.5161235	3.931118	-2.3321550	-2.6466258	0.2392657	0.0812111
Healthy-T4 - Moderate	-1.2883863	0.4950251	3.328420	-2.6026689	-2.7793867	0.2026140	0.0721083
Healthy-T4 - Severe	-1.3641185	0.5520604	5.138385	-2.4709588	-2.7718161	0.0435792	0.0551466
Healthy-T4 - Follow-Up	-2.3815390	0.4817437	2.983964	-4.9435814	-3.9193340	-0.8437440	**0.0160801**
Possible - Mild	-0.0738181	0.5426574	5.030827	-0.1360308	-1.4661962	1.3185600	0.8970728
Possible - Moderate	-0.1585244	0.5226311	4.332878	-0.3033198	-1.5666558	1.2496071	0.7756590
Possible - Severe	-0.2342565	0.5769438	6.408227	-0.4060300	-1.6244713	1.1559582	0.6979334
Possible - Follow-Up	-1.2516771	0.5100691	3.934467	-2.4539364	-2.6772072	0.1738531	0.0711990
Mild - Moderate	-0.0847063	0.4819154	250.291870	-0.1757700	-1.0338324	0.8644199	0.8606167
Mild - Severe	-0.1604384	0.5468912	227.811826	-0.2933644	-1.2380502	0.9171734	0.7695107
Mild - Follow-Up	-1.1778589	0.4195417	259.735224	-2.8074895	-2.0039951	-0.3517228	**0.0053716**
Moderate - Severe	-0.0757321	0.5266031	227.107308	-0.1438125	-1.1133849	0.9619206	0.8857760
Moderate - Follow-Up	-1.0931527	0.3905683	250.001722	-2.7988772	-1.8623763	-0.3239291	**0.0055279**
Severe - Follow-Up	-1.0174206	0.4850365	261.755451	-2.0976166	-1.9724905	-0.0623506	**0.0368981**